

高抒, 贾建军, 杨阳, 等. 陆架海岸台风沉积记录及信息提取[J]. 海洋学报, 2019, 41(10): 141–160, doi:10.3969/j.issn.0253-4193.2019.10.009
Gao Shu, Jia Jianjun, Yang Yang, et al. Obtaining typhoon information from sedimentary records in coastal-shelf waters[J]. Haiyang Xuebao, 2019, 41(10): 141–160, doi:10.3969/j.issn.0253-4193.2019.10.009

陆架海岸台风沉积记录及信息提取

高抒¹, 贾建军¹, 杨阳¹, 周亮¹, 魏稳¹, 梅衍俊¹, 李亚南¹,
王黎¹, 赵培培¹, 刘桢峤¹, 张丽芬¹

(1. 华东师范大学 海洋科学学院 河口海岸学国家重点实验室, 上海 200241)

摘要: 长时间尺度风暴强度-频率关系与气候变化相关联, 而器测记录和历史记载难以提供充分的信息, 因此从沉积记录中提取风暴信息成为一个前沿科学问题。在应用上, 这项研究可为海岸带城市群应对未来气候和海面变化提供决策依据。本文回顾了台风沉积记录研究进展, 显示陆架泥质沉积、海滩及海岸沙丘、潮滩、潟湖、巨砾是台风事件记录的良好载体, 可通过层序形态和物质特性分析而识别。同时, 还需进一步完善分析方法, 以区分台风、冬季风暴、河流洪水和海啸等不同类型的极端事件沉积。在台风强度信息提取方面, 陆架泥质沉积所含贝壳-粗颗粒沉积物可作为海底再悬浮强度的指标, 但需更多实测数据的率定; 海滩及海岸沙丘顶部的台风沉积分布高程指示了台风激浪流的上冲高度, 而台风巨砾的重量可以与近岸波浪的波高建立联系。以上数据经过换算后可以得出台风强度的信息, 虽然这些间接的沉积学信息还不足以建立风暴强度-频率关系, 但有助于台风强度大数据的建立。潮滩、潟湖沉积连续性好, 可构成台风事件的时间序列, 然而关于台风强度却是多解的, 台风最大风力、持续时间、移动路径、登陆地点的不同组合可能产生同样的事件沉积。我们建议, 应发展台风信息提取的新方法, 来解决这个问题。进行现代过程模拟, 根据已知的台风事件资料构建沉积物输运堆积模型, 使之能够复演事件沉积的特征; 进行多个地点事件沉积的反演模拟, 在此情形下, 即便每个站位的结果是多解的, 但针对多个站位上求取其解的交集之后, 多解性将下降, 这种模拟方法可称之为“解空间收缩法”; 采用大数据融合方式, 将其他来源的台风强度数据纳入模拟体系, 可进一步降低风暴信息提取的不确定性。动力过程模拟与大数据融合方法的建立, 有助于获得与沉积记录同样时间尺度的台风强度-频率关系曲线, 进而分析台风动态与气候变化的关系。

关键词: 台风过程; 事件沉积记录; 频率-强度关系; 沉积动力过程模拟; 解空间收缩法; 陆架海岸

中图分类号: P736.21; P732.5

文献标志码: A

文章编号: 0253-4193(2019)10-0141-20

1 引言

事件沉积是极端环境过程的产物, 有风暴、海啸、浊流、崩塌等沉积类型。其中风暴沉积与热带气旋、冬季寒潮、龙卷风等过程相联系。热带气旋产生于热带、亚热带洋面(5°~20°N, 5°~20°S), 在全球有多个发源地^[1](图 1)。在西北太平洋区域形成者称作台风, 在大西洋或北太平洋东部发生者称为飓风, 而

在南半球发生者则称为旋风。西北太平洋是全球发生热带气旋最多的区域之一, 全球每年约 1/3 的热带气旋产生于该区域^[3]。

热带气旋按底层中心附近最大风力可划分为 6 个等级, 热带风暴级别(最大风速 17.2~24.4 m/s)或更强的热带气旋可引发灾害事件, 给生命财产带来重大损失^[4-7]。由于人口和社会财富日益向海岸带集中, 如今同样强度的灾害可能造成加倍的损失, 这就

收稿日期: 2019-07-02; 修订日期: 2019-07-30。

基金项目: 国家自然科学基金重点项目——海岸风暴频率-强度关系的沉积记录分析(41530962)。

作者简介: 高抒(1956—), 男, 浙江省杭州市人, 教授, 主要从事海洋沉积动力学和沉积地质学研究。E-mail: sgao@sklec.ecnu.edu.cn

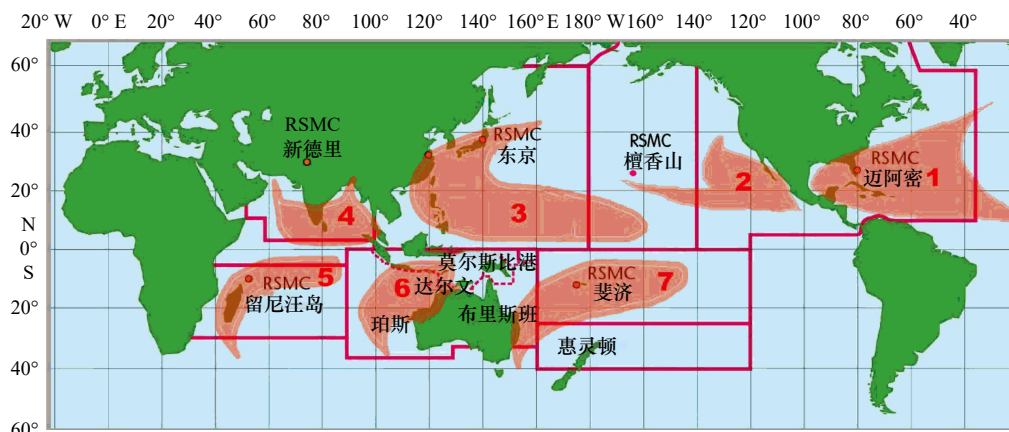


图 1 全球台风发源、生长区分布^[2]

Fig. 1 Global distribution of tropical cyclone source areas^[2]

1. 大西洋(包括北大西洋、墨西哥湾和加勒比海); 2. 东北太平洋(由墨西哥至日期变更线); 3. 西北太平洋(由日期变更线至亚洲包括南海); 4. 北印度洋(包括孟加拉湾和阿拉伯海); 5. 西南印度洋(非洲至 100°E); 6. 东南印度洋/澳大利亚(100°~142°E); 7. 澳大利亚/西南太平洋(142°E~120°W); RSMC 表示区域性专职气象中心

1. Atlantic basin (including the North Atlantic, the Gulf of Mexico, and the Caribbean Sea); 2. northeast Pacific Ocean (from Mexico to the International Date Line); 3. northwest Pacific Ocean (from the International Date Line to Asia, including the South China Sea); 4. north Indian Ocean (including the Bay of Bengal and the Arabian Sea); 5. southwest Indian Ocean (from Africa to 100°E); 6. Southeast Indian Ocean/Australia (100°E to 142°E); 7. Australia/Southwest Pacific Ocean (142°E to 120°W); RSMC denotes Regional Specialized Meteorological Center

对海岸防护提出了新要求。此外,在全球气候变化背景下,特定强度事件的重现期会变得不准确,这进一步提高了防范未来极端事件的难度。

以往海岸防护工程设计是根据器测时代(百年尺度)的频率-强度曲线来确定的,气候和海面变化因素未能充分考虑。利用沉积记录,能够将时间尺度延伸到 $10^3\sim 10^4$ a,可提高极端事件强度-频率曲线的预测能力。在浅海陆架^[8]、潮滩^[9-12]、潟湖^[13-14]、滨海沼泽湿地^[15]等环境中可形成多种类型的风暴沉积。由此引发的关键科学问题是识别出风暴沉积之后,如何提取形成过程信息,并使之与表征风暴特征参数(如台风最大风力、持续时间、移动路径和登陆地点等)相联系。

本文试图总结西北太平洋地区的陆架海岸台风沉积记录及其信息提取的研究进展,包括台风沉积记录类型和辨识、台风过程信息的提取方法、与其他类型极端事件沉积的区分、沉积记录指示的台风活动与气候变化关系等主题。在归纳前人研究的基础上,提出新的科学问题和研究建议。由于台风沉积与一般风暴沉积之间存在着共性,因此本研究也部分涉及了其他区域的风暴沉积特征。

2 西北太平洋区域台风及其沉积环境影响概况

2.1 台风形成与沉积过程观测

台风形成、发展需要 3 个必要条件^[16-19](图 2)。

首先,台风初始形成需要有广阔的海面和高温、高湿的大气环境。气温、水温较高的海域,海面蒸发量大,造成低层大气不稳定性层结;一般而言,台风源区从海表至 60 m 深度内的海水水温都要高于 $26\sim 27^\circ\text{C}$ 。其次是大气的正反馈机制。低层大气出现辐合气流,气块抬升至对流高度以上,释放出凝结潜热,加热大气并导致气流持续上升,地面气压继续下降,辐合气流可进一步加强,促进台风的形成。地转偏向力使辐合气流形成逆时针旋转的水平涡旋,在纬度大于 5° 的低纬地区比较合适。最后,台风源区的对流层风速垂直切变要小,这样对流层上下的空气相对运动较弱,释放的凝结潜热被用于加热同一个气柱,因此可以很快形成暖心结构,使中心气压降低。

台风低层结构早在 1860 年已为人所知,对其高层结构的了解则得益于雷达观测。早期台风观测来源于船舶记录和陆地台站资料,1936 年全球无线电探测网的建立,使得台风高空观测成为可能。1955 年,第一个以观测台风为主要目标的沿海雷达观测网在美国建立。1960 年,泰罗斯一号卫星拍摄到第一张关于台风的卫星照片,卫星探测台风从此拉开了序幕^[19]。随着空间科学技术的发展,各种卫星遥感技术相继应用于台风观测。

台风沉积动力过程的现场观测难度很大,台风发生时安装于浅海、近岸水域的仪器安全往往难以保障,只有在局部地点(如潮滩)能够进行全潮水文观测

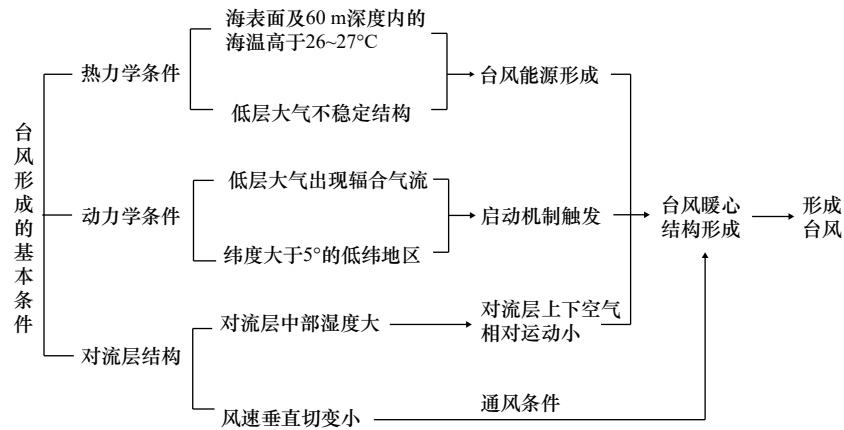


图2 台风形成的基本条件示意图

Fig. 2 Schematic diagram of basic conditions for typhoon formation

(图3), 实施水位、波浪、潮流、悬沙浓度和床面高程的高频记录^[20]。因此, 人们经常在台风事件前后进行短柱样采集, 分析沉积物的粒度分布、地化元素等物性指标的变化。

2.2 台风移动路径、持续时间、频率和强度

西北太平洋台风路径复杂多变^[22], 可分为4类^[23](图4)。第一类在菲律宾东部形成, 向NW-N移动,

其中约75%登陆东亚(中国大陆、台湾、韩国、日本); 第二类台风的源地更偏西, 或位于南海, 生成后向W-NW移动, 其中97%登陆东南亚(菲律宾、越南)或华南地区; 第三、第四类台风源地比前两类更偏东, 通常只停留在开阔的洋面上, 登陆可能性低^[23]。

西北太平洋台风有明显的季节和年际变化。1-4月台风最少, 仅占一年总数的7%, 风速也最小; 7-9月台风最多, 频率占总数的66%; 10-12月的台风风速最大^[24]。随着季节变化, 台风源地位置也随之改变, 在1-4月比较偏南和偏东, 5-6月向北移动, 7-9月源地范围最广, 10-12月向南移动。从年际变化来看(图5), 台风频次和持续时间分别呈现30 a (1960-1990年和1990-2017年)和5~10 a的周期性变化。过去几十年以来, 台风有发生频率降低、强度增高的趋势^[24-27]。

基于器测记录的理论^[28]和模拟^[29]研究表明, 随着全球气候变暖, 海表温度的升高, 本区域台风强度应提高。未来热带气旋全球平均频率将下降6%~34%, 但是台风生长周期变长、强度变大^[28], 伴随着台风中心附近降水的增加^[30]。

2.3 台风记录

西北太平洋海域台风器测时间较短, 气象观测记录到的最早台风是1881年南海“8号”台风。历史文献资料具有很高的时间准确度和分辨率, 已有学者用来重建过去几百年间易受台风影响的中国、日本和菲律宾等国家和地区的台风活动^[31-33]。我国的历史资料保存得较为完好, 有2000多年的天气和气候记录, 且近1000 a来的记录基本连续^[34], 尤其是地方志记载的台风信息较全^[35-38]。中国历史文献记载的最早台风登陆时间是公元816年, 登陆地为山东密州(今高密)^[39]。学者们利用此类资料重建了华东沿

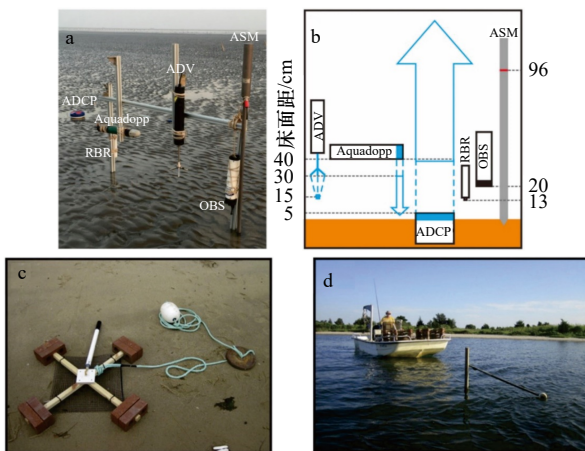


图3 现场观测仪器架设方案

Fig. 3 Instrument deployment for in site observations

a和b为潮滩观测常规仪器, RBR观测水位、有效波高、有效波周期, ADCP和Aquadopp观测剖面流速, ADV观测定点三维流速和底部高程, OBS观测定点悬沙浓度, ASM观测剖面悬沙浓度。

c和d分别为潟湖水文观测的流速仪和水位仪(修改自文献^[20-21])

a and b are conventional instruments for tidal flat observation including RBR (water level, significant wave-height, significant wave-period), ADCP and Aquadopp (current velocity profile), ADV (3d velocity and bed level), OBS (suspended sediment concentration) and ASM (suspended sediment concentration profile); c is current meter for lagoon environment observations; and d is water level gauge (modified from references^[20-21])

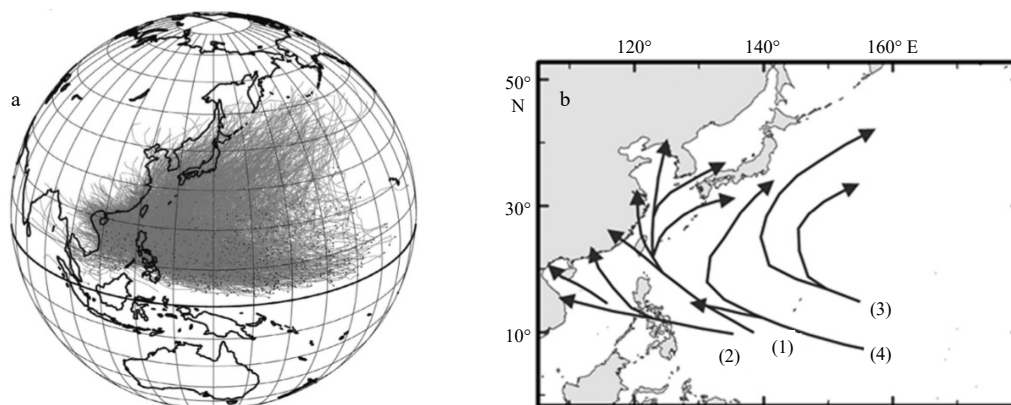


图4 西北太平洋台风特征

Fig. 4 Typhoon characteristics in the Northwest Pacific region

a 为 1945–2010 年台风路径图(灰色线条是台风路径,黑点是台风源地,修改自文献 [22]); b 为台风路径分类简图: (1) 代表 NW-N 向移动, 主要登陆东亚地区, (2) 代表 W-NW 向移动, 主要登陆东南亚和我国华南地区, (3) 和 (4) 代表 NW-NE 向移动, 较少登陆(据文献 [23] 绘制)

a is typhoon tracks from 1945 to 2010 (gray lines indicate the typhoon tracks and the black points indicate typhoon genesis, modified from reference [22]); b is four types of typhoon tracks: (1) represents typhoons traveling towards NW-N, with around 75% of them causing landfall over East Asia, (2) represents typhoons moving towards W-NW, with 97% of them striking Southeast Asia and/or southern China, and (3) and (4) represent typhoons moving towards NW and NE, with a small probability of reaching land (modified from reference [23])

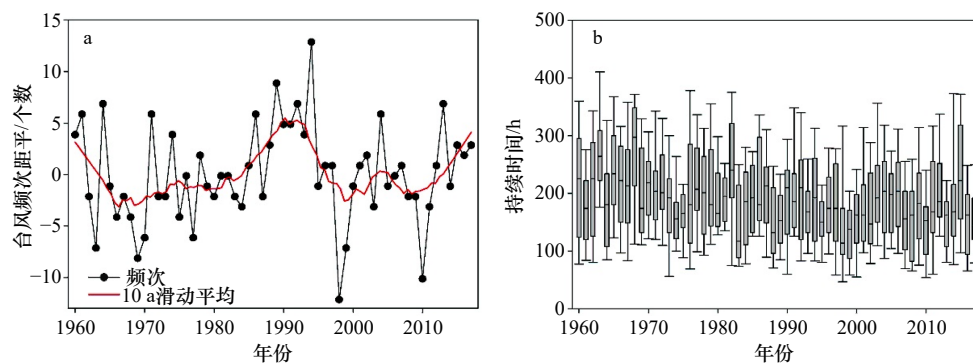


图5 1960–2017年西北太平洋台风频次和持续时间年际变化特征

Fig. 5 Interannual variations of frequency and duration of typhoons in the western Pacific from 1960 to 2017

a. 台风频次; b. 持续时间

a. Typhoon frequency; b. duration of typhoon

海[40–42]、华南[31, 38, 43–44]等地区的古台风记录, 获得了日本历史时期的台风路径和规模信息[45–46], 重建了菲律宾群岛的风暴年代序列、并区分了台风事件和热带风暴[32]。此外, 基于历史资料及器测记录的结合, 探讨了太阳活动[22]、厄尔尼诺(El Niño)强度[47]与台风发生频率的关系。

2.4 风暴期间沉积物侵蚀、输运、堆积过程

风暴增水与潮波相结合, 可改变海岸沉积物的输运状态[48]。在潮滩环境, 由于台风期间底部切应力大幅提高, 水体悬沙含量和输运率可数倍甚至 10 倍于平静天气[49], 沉积物净输运可向陆[50]、向海[51], 或兼而有之[9]。台风期间, 潮滩不同部位的响应不同, 光滩在台风期常经历较常态高 1~2 个量级的侵蚀[8], 侵

蚀有时可上溯至盐沼中部和下部[9]。台风还可刷深盐沼带中零星分布的洼地, 形成冲刷坑[52], 或导致植被根系出露、破坏植被根系, 引起盐沼边界的大幅后退[53]。台风过境后, 潮滩可较快恢复[11, 54], 盐沼前缘光滩的坡度可能因台风浪侵蚀而变陡[55]。

风暴作用下海滩激浪带的水流极大增强[56], 沿岸流和底部回流格局也变化很大[57]。激浪带一部分沉积物被输往或越过滩脊顶部, 另一部分被底部回流向海输运, 形成近岸水下沙坝[58–60]。根据台风浪大小的不同, 滩脊顶部可有加积和侵蚀两种地貌变化[61], 海滩对风暴的地貌响应比较剧烈[62]。

在堡岛或沙坝潟湖环境, 风暴时的增水、冲越流、水道切割作用对于地貌有很大影响[63]。潟湖内部可能

形成风暴越岸沉积^[12], 而潟湖外的物质也可通过潮汐汊道口门输运到纳潮海湾之内^[13, 21]。此外, 风浪在潟湖或海湾的风暴沉积中起着重要作用, 可以产生强烈的再悬浮, 造成沉积物在纳潮水域的重新分布。

3 陆架海岸典型环境台风沉积特征判别

3.1 台风沉积判别方法

陆架海岸环境中的极端事件过程与常态过程显著不同, 因而会在地质记录里留下印记。识别此类印记的原理是, 在常态过程作用下必然形成特定的沉积相, 与之进行对比, 可以发现极端事件沉积的典型特征^[64](图6)。例如, 在内陆架泥质沉积中出现砂层、贝壳层, 很可能是非常态过程的产物。风暴沉积在不同的海岸环境^[69]和同一环境中的不同部位^[70-71]有很大的差异。由于沉积相的刻画是以沉积层的形态(如层理)和物质特性(如粒度和物质组分)为指标

的, 因此极端事件沉积也有其形态和物性两方面的特征指标。

对于潮间带至大陆架范围内的浅海水下沉积, 由于台风浪引发的振荡流存在, 所形成的圆丘状交错层理是风暴沉积记录的重要指标^[72]。对于海岸沙滩、潟湖等环境, 风暴事件沉积层一般可通过以下特征进行识别和验证^[73-75]: 向陆变薄的砂层、贝壳层; 具区域性的生物扰动痕迹; 古海洋生物化石, 如有孔虫、孢粉等; 含量相对较低的铁、钛等陆源元素和较高的钙、锶等海源元素(图7); 较高的¹³C和¹⁵N含量等。

上述指标的分析方法与沉积学方法是一致的。粗颗粒沉积物的识别方法主要有光学摄像法、X射线拍摄法和粒度分析法; 由于外界环境的扰动作用和细颗粒背景沉积物的影响, 光学图像具有不确定性, 但粒度参数和通过X射线得到的灰度值却可以清楚识别粗颗粒沉积物^[75]。颗粒物组成方面的指标可用矿物学、微体古生物学方法来确定。地球化学组

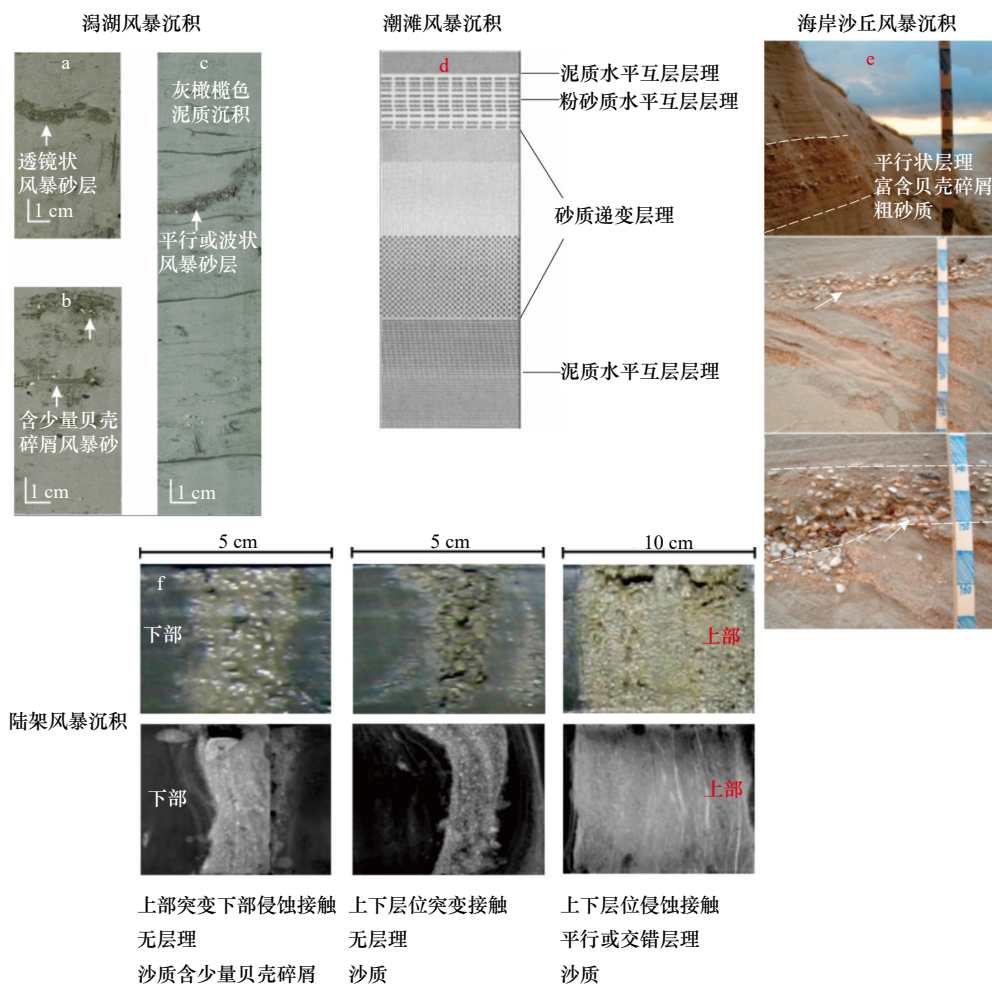


图6 潟湖(a, b, c)、潮滩(d)、海岸沙丘(e)和陆架(f)环境下典型台风沉积的垂向序列(修改自文献[65-68])
 Fig. 6 Vertical sedimentary sequence of typical typhoon deposition in lagoons (a, b, c), tidal flats (d), coastal dunes (e) and shelves (f) (modified from references [65-68])

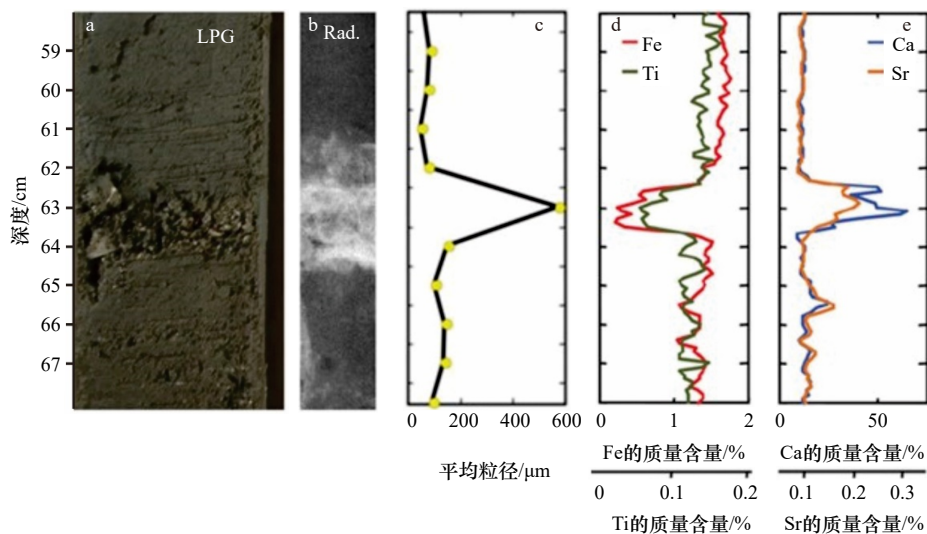


图 7 风暴沉积的岩芯光学图像(a)、X 射线照片(b)、粒径分析图(c)和 X 射线荧光光谱图(d, e)

Fig. 7 Optical image (a), X-radiograph (b), grain-size (c) and X-ray fluorescence (d, e) from representative storm deposits

X 射线照片白色层为砂砾质物质, 深灰色层为细颗粒沉积物(据文献 [75] 改绘)

For X-radiographs, white layer represents coarse-grained, dense sandy material and black layer represents fine-grained, organic-rich fair-weather, backbarrier deposits (modified from reference [75])

分可通过 X 射线荧光光谱分析法(XRF, 图 7)、有机地球化学分析等方法来测定^[7]。

3.2 陆架泥中的台风沉积

全新世陆架泥质沉积区具有环境稳定、沉积记录连续的特点^[76]。风暴事件沉积在泥区差异性突出, 风暴过境期间的强降水带来陆源沉积物, 而风暴浪可使底层发生再悬浮, 连同部分陆源物质随离岸流向海外扩散输运^[77], 形成侵蚀面和物质粗化。在元素地球化学方面, 通常表现为 SiO_2 含量增大、 Al_2O_3 的含量降低、Zr/Rb 比值上升和 Sr 元素含量增加等特点^[78]。由于台风期间较细沉积物可输运得离岸线更远, 风力衰减后沉积物粒度逐渐减小, 因此台风沉积在整体上还呈现出向海变薄、向上变细的特征^[7]。陆架泥台风事件年代测定, 一般可采用 ^{210}Pb 、 ^{137}C 、AMS ^{14}C 和光释光方法。

浙闽沿岸泥对长江入海物质变化较为敏感^[79-80], 但其沉积物类型总体上是稳定的。由于泥质区顶部水深较小, 因此台风期间海底易遭受冲刷, 蚀余物质为贝壳碎屑和砂质物质, 在过去 2 000 a 的泥质沉积中含有多层此类沉积^[81]。台风期间的观测数据表明, 再悬浮作用可形成底部浑浊层, 并以陆架重力流的方式向海方向运动^[82]。以粗颗粒物为标志的台风沉积已得到研究者的认同, 而风暴形成的底部浑浊层堆积体尚待深入研究。浙闽沿岸泥向海一侧的沉积构造表现为向海平行推进的斜坡沉积, 被认为是沉积物重力流的标志^[83], 因此如何区分台风成因的和其他

成因的陆架重力流堆积, 也是尚待研究的问题。

3.3 潮滩台风沉积

高能事件下, 潮滩表面水动力及其沉积物输移格局均发生显著变化, 形成的潮滩沉积将明显区别于正常条件下的沉积产物。台风期伴随强烈的滩面侵蚀, 可形成侵蚀底面; 底面以上的台风期沉积物颗粒较粗而分选较差, 自下而上逐渐变细; 沉积层序常为下部充填粗颗粒沉积、上部具有纹理的二元结构^[71, 84-85]。然而, 上述模式可能只适用于潮滩中下部, 潮滩上部也可能缺失侵蚀底面^[86], 而快速沉积层序中沉积物粒度的垂向差异可能并不显著^[87]。因此, 台风沉积层序要区分潮滩的上部、中部、下部或潮下带^[88]。江苏潮滩沉积的研究表明, 台风沉积可以是加积或蚀余性质的, 表现为潮滩的上部堆积而下部侵蚀^[89]。潮滩上部的沉积层保存潜力最高, 在垂直于岸线方向设置柱状样断面、使各个样品首尾相接, 可获得连续的沉积记录^[90]。此外, 为了合理分析潮滩下部沉积所含的台风记录, 可对同时形成的潮间带上下部事件沉积进行对比, 从而利用潮滩上部数据厘定下部数据, 校正台风发生频率信息。

3.4 海岸潟湖台风沉积

一般而言, 潟湖水动力较弱, 沉积物以富含有机质的细颗粒物质为主。风暴增水和风暴浪常常携带沉积物越过堡岛, 在其向陆一侧的潟湖边缘形成冲越扇沉积, 其物质主要来自海滩和堡岛表层的粗颗粒陆源物质或生物碎屑, 它们与富含有机质的暗色细颗粒

沉积物具有鲜明的差异,通过沉积学、地球化学等分析可有效识别出来^[4, 13, 91]。Sr 元素峰值^[12]、生物指标^[92-93]等都是潟湖风暴沉积层鉴别的常用指标。以上分析方法必须满足一定的假定条件,即堡岛高程和地貌在有风暴记录的时间尺度内基本保持不变^[94]。

另外,台风登陆时往往带来短时高强度降雨,容易引发海岸地带局域洪水,携带大量粗颗粒沉积物注入到附近的海湾或潟湖中。流域洪水沉积和潟湖沉积中有机物质及其同位素存在的显著差异,为利用潟湖流域洪水沉积重建古台风事件序列提供了可能^[95],重建结果与历史文献记载也有较好的对应^[96]。然而,在 $10^2\sim 10^4$ a的时间尺度上,流域洪水沉积可能有两种成因,除了台风带来的极端降水之外,也有可能是季风降水形成的局域洪水事件,因此还需要其他资料的印证来进行甄别。

3.5 海滩与海岸沙丘台风沉积

台风在海滩剖面演化中具有重要作用, Sallenger^[63]将台风对海滩的影响分为4个等级:在冲击和碰撞影响模式下,海滩剖面主要以侵蚀特征为主,台风过后,海滩剖面逐渐恢复;如果波浪爬高或台风潮水位超过海滩顶部高度,就会发生冲越流越过海滩顶部而在海滩后部及以上位置形成冲越沉积物^[97],其特点是由极高能量驱动的快速沉积物运动,通常覆盖于海岸沙丘上。

激浪带附近滩面在台风之后容易恢复,并且还有年周期地貌变化^[98],因此这里的台风沉积记录难以保存。相对而言,滩脊和海岸沙丘顶部的冲越沉积是台风影响海滩的重要证据,可以指示台风的持续时间、影响范围和环境条件^[99]。

冲越沉积有两种情形。当台风相对较弱,沙丘顶部地势较高,冲越沉积仅能覆盖于滩脊或沙丘与海滩的过渡地带;如果台风非常强大,波浪流运输的物质将翻越顶部,可在沙丘背后形成冲越扇^[100]。由于海岸沙丘形态、植被覆盖和沉积物特征的不同,不同地方的冲越沉积特征亦有区别^[101]。上述第一种类型指示了台风期间的最大影响高度,因而可据此推算波浪冲越高度,获得台风强度信息^[102]。

3.6 海岸巨砾

海岸巨砾是海岸带珊瑚礁或砾质海岸被巨浪推送上岸的巨大块体,因保存潜力高、体积大、易识别,是研究长周期极端水文事件的良好载体^[103-105](图8);按成分可分为钙质(珊瑚礁块)和硅质(基岩岩石)巨砾,按照成因则可分为风暴巨砾和海啸巨砾。风暴巨砾最重可达 10^2 t^[105, 108],海南岛小东海的珊瑚礁台风巨砾(图9)形态不规则,三轴长度为 $10^{-1}\sim 10^0$ m量级。

结合动量方程和波浪运动方程,已重构了台风巨砾在极端水文情况下所受到的水流作用和搬运距离^[109],并反演了当时的台风强度^[103, 110-111]。这些重建工作依赖于巨砾参数的精确提取。近年来,三维激光扫描^[112-114]、无人机和卫片^[115-116]以及射频识别^[117]等新技术提升了巨砾形态的研究精度。此外,数值模拟有助于确定巨砾沉积所需的风浪强度^[118-119],并进而推算台风强度。徐笑梅等^[120]根据海南岛东北部海岸的硅质巨砾的重量和分布位置,推算了波浪强度,并由此证实该巨砾沉积是强台风所致。

台风巨砾研究的难点在于如何确定台风发生的时间。巨砾数量虽多,但由于缺失年代数据而无法构成台风事件的时间序列。珊瑚礁巨砾年代信息的获

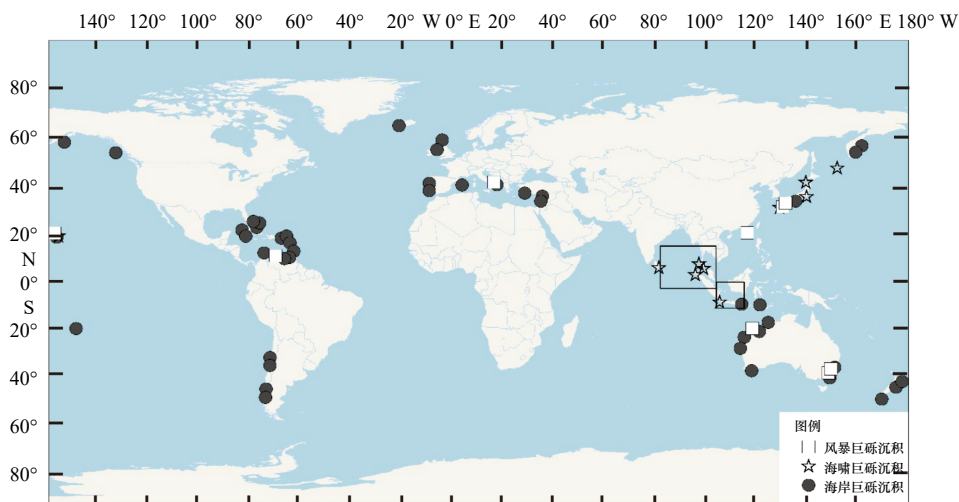


图8 世界范围内已发现的不同成因的海岸巨砾沉积(改绘自文献[106-107])

Fig. 8 Global distribution of coastal boulders with different causes (modified from references [106] and [107])



图9 典型台风巨砾沉积(摄于海南岛小东海)

Fig. 9 Typical typhoon boulder deposits (Xiaodonghai, Hainan Island)

取不能以礁体本身的年龄为准,此年龄只能代表形成巨砾的台风事件的时间上限。巨砾所在的位置也能提供一定信息,如果巨砾堆积后不再移动,那么所处的礁平台位置提供了另一个独立的年代上限:依据珊瑚礁平台地貌演化模式,可确定所在位置的形成时间。巨砾暴露于陆地环境,必定受到陆上环境的影响,因此雨淋、附着生物、磨蚀等过程也可能提供年龄和是否曾被翻动的信息。

4 讨论

4.1 台风暨风暴沉积记录的完整性和保存潜力

任何孤立地点的事件沉积都很难完整记录台风过程,一方面受到台风移动路径以及台风强度大小的制约,另一方面受沉积层保存潜力的影响。

保存潜力与沉积速率、地貌稳定性、水动力条件、生物扰动和沉积物供应等因素有关^[75, 90, 121-122]。沉积速率过低的沉积环境,作为风暴沉积特征的粗颗粒物不能较快地埋藏,易受到后续侵蚀和再搬运的影响。在相对稳定的环境,如海岸潟湖和盐沼,风暴沉积得以保存的概率较高。低能量的水动力环境可免遭潮流改造,若流速较大,沉积体可被迅速侵蚀或混合^[121, 123]。弱潮海岸的潟湖和海湾受潮汐、波浪影响相对较小,保存潜力较高^[13, 124]。高能环境下的海滩、沙坝沉积中风暴沉积的保存潜力较低^[125]。

沉积物供应状况影响宏观的冲淤趋势。例如,沙坝潟湖环境的沉积物供应不足,可能导致沙坝宽度减小,因而台风浪越顶事件就更容易发生,并在潟湖中堆积风暴越岸沉积;相反,若沙坝持续生长向海推进,甚至封闭口门,沙坝后潟湖对风暴响应的敏感程度就会降低^[126]。对于盐沼环境,由于生物的扰动混合作

用,可能造成沉积环境和沉积记录的错误解释^[122]。

为了获取长时间尺度的连续台风沉积记录,沉积体系的完整性和保存潜力是必须考虑的重要因素。在前述台风沉积的载体中,潮滩、潟湖沉积连续性好,可构成台风事件的长时间序列。

4.2 风暴沉积记录的沿岸分布及信息差异

陆架海岸台风和其他风暴沉积记录分布于不同的环境,包括浅海陆架^[127-128]、堡岛-潟湖^[64, 129-130]、珊瑚礁平台^[47, 131-132]、滩脊-海岸沙丘^[102, 133-134]、三角洲-河口湾^[85, 135]和潮滩^[10, 136]等。这些环境中的台风信息有很大差异。

浅海陆架的风暴沉积以侵蚀面、砂-泥单层交互和波状起伏交错层理为特征^[127, 137]。一般来说,越靠近海岸,整个沉积剖面的风暴沉积所占比重越大,风暴沉积层越多且单层厚度越大^[128]。

滨岸湖沼相的冲越沉积研究始于墨西哥湾沿岸^[129],是目前全球古风暴学研究中应用最为广泛和成熟的地质记录^[4, 12, 138]。那里堡岛陆侧发育潟湖,正常天气时沉积环境稳定,以泥质沉积为主且富含有机质;风暴增水和风暴浪携带沉积物在堡岛陆侧形成冲越沉积,以浅色粗颗粒、低有机质含量和 Sr 元素高含量为特征^[12]。

对于海滩-珊瑚礁海岸系统,每次风暴都可能产生一系列沉积,如潟湖沉积、滩脊、海岸沙丘顶部沉积、风暴巨砾等。风暴发生时,粗颗粒沉积物会通过波浪越顶、口门水道、陆域洪水等途径输运到潟湖中并堆积下来,使沉积物粗化、有机质含量锐减、碳酸盐含量增加^[47]。通常认为,相对高陡的滩脊(高出海平面 2~6 m)由风暴形成,含有大量贝壳碎屑;风暴沙脊高度可用于估算古风暴强度^[134, 139]。发育在泥质海岸的贝壳堤,可能指示台风比较活跃的时期^[140-141]。岩块或者珊瑚礁块堆积为风暴巨砾,指示了风暴浪的强度^[142-143]。海岸沙丘陆侧的越顶沉积,可用于确定风暴浪强度的下限^[102, 144]。

大河三角洲地区,河口、潮滩、潮流三角洲、沿岸泥区等环境中形成的沉积记录仍然可以达到年代际或更高的分辨率^[7, 10, 85, 145-146]。河口地区洪水、潮汐作用相对较强,因此在风暴强度信息提取时应给予考虑。

由于不同环境的差异,事件沉积是多样化的,与台风强度的关系也不同。因此,在台风登陆地区,沉积环境和事件沉积记录的多样性对台风信息提取研究是有利的。多种数据可形成相互独立的证据,提高台风强度判别的准确性。同时,分布于大范围的同时事件沉积,可形成空间上完整的台风记录。今后,应

对重点区域进行所有台风沉积记录集成工作,成为台风大数据的组成部分。

4.3 台风沉积与其他极端事件沉积的辨识

我国海岸带沉积记录含有多种事件沉积类型,除台风外,还有冬季寒潮、河流洪水、海啸等,有必要加以区分。在岩心特征上,台风与洪水、海啸等其他极端事件沉积特征有相似之处^[147]。

冬季寒潮主要影响中高纬度海岸^[148],与台风相似,也表现出增水和波浪作用加强。从寒潮与台风的持续时间的对比上,有可能建立区分指标;寒潮发生于冬季,而台风发生于夏、秋季,因此事件沉积中的季节信息也很重要。在长江口区,沉积层中的生物生长季节信息^[149]可能是适用的。

在河口三角洲区域,陆源和海源有机物质的 TOC/TN 元素比值和 C、N 稳定同位素组成有显著不同^[150]。在长江口,风暴砂层的海源性有机质含量更高,表现为 $\delta^{13}\text{C}$ 值较高和 TOC/TN 比值较低,而河流洪水沉积物颗粒较细, $\delta^{13}\text{C}$ 值较低,TOC/TN 比值较高^[5]。关于风暴和洪水共同作用下的河口极端事件沉积识别,需进行洪水前后和风暴前后沉积物对比分析^[151]。

在远离河口的低纬度海岸,海啸、台风沉积的区分已成为海岸沉积学研究的主要挑战^[152-153]。垂向沉积结构的差异是区分两类沉积的指标之一。海啸一般只经历一轮来回或者只有向岸运移的输运过程,因此海啸沉积物往往只存在 1~2 个分层结构^[152, 154-156],甚至缺失沉积结构^[157]。海啸沉积从岸线向内陆厚度逐渐变薄,颗粒逐渐变细^[158]。台风过程影响时间长,存在反复多轮的向岸运移和回流过程,因此沉积可有明显的分层结构。

从分布范围来看,海啸沉积可在海岸线向内陆 100~1 000 m 的区域内形成,海拔高度 10~100 m,而风暴沉积则限于 10~100 m 的范围,海拔高度一般只有几米^[152, 155]。2011 年日本海啸的最大爬升高度为 39.7 m,整个沿海约 425 km 海岸的海啸爬升高度超过 10 m^[158]。

地球化学指标可揭示极端事件沉积的物源^[156, 159],从而可以用来估计海啸在泥质海岸带的淹没范围。另一个潜在的方法是用沉积物中的生物 DNA 来识别是否为海啸沉积物,因为海啸沉积物中会混有外海的生物 DNA 成分^[160]。

沉积物中混杂的异常物质亦有可能指示古海啸沉积。贝壳、有孔虫壳体、植物残体、碎屑岩颗粒等是常见的夹杂物,其形态从完整到破碎均有体现,且相对比例差异较大^[161-162]。在有人类活动的地区,海

啸沉积物中还可能包含人工产物的遗迹^[157],同次海啸在西沙群岛形成的沉积则是组成单一的珊瑚砂层^[156]。

海啸可搬运重量可达 100~200 t 海岸巨砾,搬运距离可超过 500 m^[163]。1771 年日本 Meiwa 海啸将两块直径为 6 m、5 m 的海啸石分别搬运至距海岸线 1 500 m、海拔 10 m 之处^[120]。台风也可搬运 100 t 巨砾,但通常分布于珊瑚礁或海岸悬崖边缘,距岸线最远不超过 300 m^[107]。

上述方法在操作层面上有相当的难度,主要是工作量大、不确定性高。因此,有必要进一步探讨多参数、高精度的区分指标问题,以便在岩心分析框架下获得实用、可靠的指标。

4.4 台风强度-频率的沉积记录分析方法

沉积记录中风暴频率和强度信息的提取,首先要给出各个风暴层的发生时间。但在自然状况下,风暴沉积层可能由于侵蚀而缺失,或因为事件沉积叠复而误判为一次风暴的产物(图 10)。此外,台风在不同地点遗留的沉积记录不尽相同,故较为完整的风暴频率信息应基于同一区域的多个钻孔和不同类型的沉积记录,通过综合研判来获取。

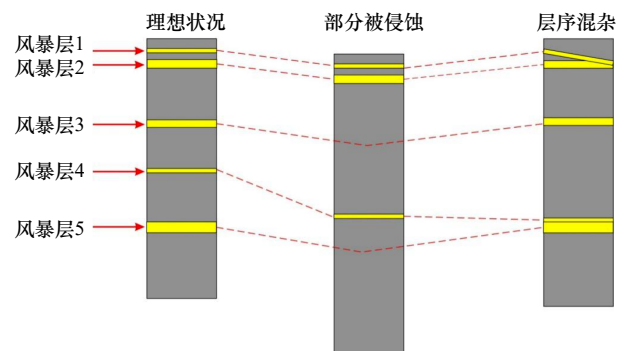


图 10 不同特征风暴沉积记录的冲淤属性示意图

Fig. 10 Diagram showing erosion and deposition properties of storm sedimentary records

目前有关风暴强度的描述主要是定性的,例如通过比较现代风暴强度和事件沉积厚度,得出了厚度越大、对应的古风暴应该越强的看法^[136, 164]。8114 号台风在江苏大丰沿海产生 11 级大风,风暴增水最高达 2.43 m;台风过后,潮上带平均淤高 0.7 cm,潮间带上部沉积的粗粉砂层平均厚 3.5 cm,潮间带中部的砂层平均厚 5.9 cm^[8]。还有学者利用现代台风在滨岸湖泊所形成的冲越扇体分布范围,大致判断形成古冲越扇的台风强度^[129],如 1979 年在亚拉巴马州登陆的飓风 Frederic 在 Lake Shelby 所形成的冲越扇只局限于

湖缘,因而推断湖中心钻孔所揭示的砂质沉积应该是更强飓风所形成的。

在频率-强度关系研究上, Elsner 等^[165]的案例较为成功,他们选择的研究地点有一个风暴强度的阈值:只有超出阈值的风暴才能形成事件沉积。在此特定地点,根据钻孔中 3 500 a 记录里含有 11 层风暴层,确定最小重现期为 318 a,使得该地区的风暴强度-频率曲线往前推进了约 200 a(图 11)。但是,这个案例 3 500 a 的沉积记录只能用以确定 300 a 左右的重现期,其信息没有得到充分利用。

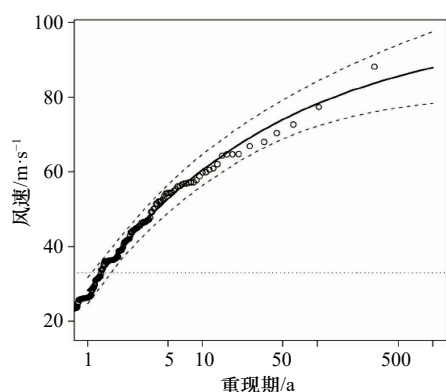


图 11 沉积记录和参数统计模型建立的台风强度-频率曲线

Fig. 11 Typhoon intensity-frequency curve based on sediment record and parametric statistical model

风速代表了台风强度,虚线为 95% 置信区间(修改自文献^[165]);只有最上端的一个数据点来自沉积记录

The wind speed represents the typhoon intensity, and the dotted lines reveal the 95% confidence interval (modified from reference^[165]). Only one data point from the top was derived from the sedimentary record

Nott 和 Forsyth^[166]根据 5 000 a 沉积记录,发现了风暴事件存在 10^3 a 尺度上的系统状态转换。Woodruff 等^[167]利用简单的平流-沉降模型来确定滨岸湖沼相的冲越沉积事件所伴随的风暴增水相对强度,并得到了广泛的应用^[130, 168]。近年来,不少研究者试图利用海岸沙丘风暴沉积和风暴巨砾记录,根据数值模型重建古风暴的强度^[102, 108, 169]。

随着模拟技术的发展, Delft3D、ROMS、MEOW 等数值模型都已尝试应用于古风暴学研究。Nott^[139]、Nott 和 Forsyth^[166]以过去风暴增水的高度和历时为输入参数,利用 MEOW 和 GCOM2D 模型来确定古风暴的强度。Brandon 等^[170]试图以模拟方法建立台风最大风速与沉积物粒径之间的关系,并重建了西北佛罗里达地区距今 2 500 a 以来的风暴强度。关于风暴沉积记录形成的模拟研究还处于起步阶段,但已展现良

好前景^[170-171]。

潮滩、潟湖沉积记录有较好的连续性,可提供台风事件的时间序列,由此可以确定台风发生频率;相对而言,台风强度信息的提取要困难得多。在这两类环境中,同一地点的事件沉积的差异未必代表台风强度的差异,任何一层风暴沉积所对应的台风强度均是多解的,台风最大风力、移动路径、登陆地点、持续时间的不同组合可能产生同样的事件沉积。因此,应发展台风信息提取的新方法,来解决这个问题。

首先,需要进行现代过程模拟,根据已知的台风事件资料构建沉积物输运堆积模型,使之能够复演一个环境内部多个地点的事件沉积特征。涉及台风作用海岸沉积物输运-堆积格局及产物差异的模型研究已经开展^[172-176],关键是要对台风中心最大风力、移动路径、登陆地点、持续时间等变量的影响进行更加深入的研究,提高模拟的可靠性。台风中心最大风力影响台风浪波高、风暴增水幅度;移动路径和登陆地点均影响风向、风速的平面分布,以及海湾、潟湖的风区大小;而持续时间影响台风浪和风暴增水作用的时段,进而影响风暴沉积层的厚度和其他特征。此外,台风过程模拟还需要考虑潮汐和径流因素。

其次,进行多个地点事件沉积的反演模拟,目的是搜索到一个能够解释所有地点事件沉积的台风事件。对台风中心最大风力、移动路径、登陆地点、持续时间等变量设置可能的变化范围,针对每个采样站位,对所有可能的变量组合实施遍历式的数值实验,找出符合事件沉积输出结果的所有变量组合,可称之为该采样站位的“解集”。在此情形下,即便每个站位的结果是多解的,但针对多个站位上求取其解的交集之后,多解性将下降,这种模拟方法可称之为“解空间收缩法”。

最后,采用大数据融合方式,将其他来源的台风强度数据纳入模拟体系,可进一步降低不确定性。大数据具有以下特点:数据的大量快速产生、大量重复记录同类型数据、数据种类的多样性、数据记录形式的多样性、数据质量的差异性。充分了解这些特征,才能从大数据中获取重要信息。台风信息记录正是具有这样的特征。如前所述,不同环境、不同部位的事件沉积种类很多,反映台风强度信息的指标具有多样性,在数值模拟的框架内,如果能融合时空上分散的各种数据,包括陆架泥、海滩及海岸沙丘、风暴巨砾等数据,台风信息的指向性就会得到加强。

4.5 基于沉积记录分析的台风动态与气候变化关系

台风活动异常是全球变暖的结果^[3],或是年代际

周期性变化^[177-178],已经成为全球气候变化研究的一个焦点。全球变暖将提高台风强度^[179-181],但出现频率如何变化却有较大的不确定性^[26,30,182-183]。

近几十年来,国内外学者运用地质记录和历史文献,对日本、渤海沿岸、长江三角洲和南海等地区进行了台风活动和气候变化关系的研究^[12,31,85,131,184-185]。研究表明,全新世气温存在明显的阶段性变化,包括大暖期、中世纪暖期和小冰期等。冷期、暖期的古台风活动信息有助于理解全球变暖背景下台风变化趋势。日本鹿儿岛潟湖风暴沉积显示古台风活动存在 $10^2\sim 10^3$ a尺度的周期性变化,但这一周期性变化与全新世气温变化周期并不相符,如6 000~4 000 a BP的全新世大暖期并未出现台风频发现象,反而是台风相对平静期^[5,12]。南海永曙礁潟湖风暴沉积的研究结果表明^[131],过去1 000 a共有6个强台风发生,其中多数发生在公元1000-1500年的中世纪暖期,少数发生在公元1500-1900年的小冰期,可见强台风频率与气温之间存在一定的相关性。然而,韩国东海岸潟湖风暴沉积^[95]和我国历史文献^[31,185]表明,小冰期期间台风活动处于频发期。近期研究指出,小冰期台风活动的空间分布可能与热带辐合区的南北移动密切相关^[185-186]。由此可见,强台风发生频率与气温变化的关系还受到其他因素的制约。

根据过去6 400 a在日本鹿儿岛的研究^[12],强台风多发期对应于强厄尔尼诺期,而少发期对应于弱厄尔尼诺期^[187]。然而,从台湾岛东北部湖泊沉积的K/Rb指标重建的过去2 000 a台风降水序列中,发现拉尼娜(La Niña)期台风数明显多于厄尔尼诺期^[96],近2 000 a中国台风记录中也发现了这个特征^[185]。上述结论与现代观测资料一致,即ENSO影响台风的生成、发展和移动路径^[2,188],但在不同地区(例如日本和中国东南沿海)的效应并不一致。此外,西北太平洋台风活动还受到太平洋涛动、西太平洋副高、洋面温度和东亚季风等多种因素的制约^[185,189-190]。

台风活动与气候变化之间的长周期关系的最终确立,依赖于高时空覆盖度和高分辨率古台风沉积记录的重建。加强长时间尺度的区域性和全球性古风暴空间分异性研究,需要深入研究沉积记录所含不同阶段的台风强度-频率关系。

5 结语

迄今为止,关于台风沉积识别和台风强度信息提取的研究已经取得了一些进展,并引出了“长时间尺

度台风强度-频率关系”研究方向的新问题,总结如下。

(1)陆架泥质沉积、海滩及海岸沙丘、潮滩、潟湖、风暴巨砾是风暴事件记录的良好载体,事件沉积可通过层序形态和物质特性分析而识别。我国沿海台风沉积已被大量发现,但如何高效区分台风、冬季风暴、河流洪水和海啸等不同类型的极端事件沉积,还需寻找更多的新指标,以表征极端事件的局域性、季节性、动力过程和物源特点。

(2)台风强度信息提取方面,陆架泥质沉积所含贝壳-粗颗粒沉积可作为海底再悬浮强度的指标,海滩及海岸沙丘顶部的台风层分布高程指示台风期间激浪流的上冲高度,而风暴巨砾重量则指示了近岸波浪的波高。以上数据可经过换算得出台风强度信息。由于不同环境的差异,事件沉积是多样化的,与台风强度的关系也不同。因此,需要针对各种台风沉积来分析台风的强度和年代信息,集成所有台风沉积记录并构建台风大数据管理与分析系统。

(3)潮滩、潟湖沉积连续性好,可构成台风事件的时间序列,然而关于台风强度却是多解的,台风最大风力、移动路径、登陆地点、持续时间的不同组合可能产生同样的事件沉积。应发展台风信息提取的新方法来解决台风强度的多解性难题。一是进行现代过程模拟,根据已知的台风事件资料构建沉积物运输堆积模型,使之能够复演事件沉积的特征;二是发展解空间收缩法,进行多个地点事件沉积的反演式模拟;三是采用大数据融合方式,将多来源的台风强度数据纳入模拟体系。这种动力过程模拟与大数据融合方法的建立,有助于获得长时间尺度台风强度-频率关系曲线。

(4)台风活动与气候变化之间的长周期关系的最终确立,依赖于高时空覆盖度和高分辨率古台风沉积记录的重建。为了弄清长时间尺度的区域性和全球性古风暴空间分异性,需要深入研究沉积记录所含不同阶段的台风强度-频率关系。

致谢: 中国科学技术大学孙立广教授组织了南海暨南海岛屿环境、气候与灾害研讨会(合肥,2015年4月12-13日),并在会议期间与本文第一作者讨论了南海风暴沉积问题,之后又共同讨论了台风与海啸沉积的分辨问题。台湾大学海洋系陈惠芬教授在南海台风沉积分析上提出了建议,并提供相关资料。谨致谢忱。

参考文献:

- [1] Holland G J. Global Guide to Tropical Cyclone Forecasting[M]. Switzerland: World Meteorological Organization, Geneva, 1993.
- [2] NOAA. Subject: F1 What regions around the globe have tropical cyclones and who is responsible for forecasting there?[EB/OL]. (2014)[2019-05-30] <https://www.aoml.noaa.gov/hrd/tcfaq/F1.html>.
- [3] Elsner J B, Liu K B. Examining the ENSO-typhoon hypothesis[J]. *Climate Research*, 2003, 25: 43-54.
- [4] Emanuel K. Increasing destructiveness of tropical cyclones over the past 30 years[J]. *Nature*, 2005, 436(7051): 686-688.
- [5] Donnelly J P, Woodruff J D. Intense hurricane activity over the past 5, 000 years controlled by El Niño and the West African monsoon[J]. *Nature*, 2007, 447(7143): 465.
- [6] 廖淦标, 范代读. 全球变暖是否导致台风增强: 古风暴学研究进展与启示[J]. *科学通报*, 2008, 53(19): 2907-2922.
Liu K B, Fan Daidu. Perspectives on the linkage between typhoon activity and global warming from recent research advances in paleotempestology[J]. *Chinese Science Bulletin*, 2008, 53(19): 2907-2922.
- [7] Vecchi G A, Villarini G. Next season's hurricanes[J]. *Science*, 2014, 343(6171): 618-619.
- [8] Tian Yuan, Fan Dejiang, Zhang Xilin, et al. Event deposits of intense typhoons in the muddy wedge of the East China Sea over the past 150 years[J]. *Marine Geology*, 2019, 410: 109-121.
- [9] 任美镔, 张忍顺, 杨巨海, 等. 风暴潮对淤泥质海岸的影响——以江苏省淤泥质海岸为例[J]. *海洋地质与第四纪地质*, 1983, 3(4): 1-24.
Ren Meie, Zhang Renshun, Yang Juhai, et al. The influence of storm tide on mud plain coast—with special reference to Jiangsu Province[J]. *Marine Geology & Quaternary Geology*, 1983, 3(4): 1-24.
- [10] Yang Shilun, Friedrichs C T, Shi Zhong, et al. Morphological response of tidal marshes, flats and channels of the outer Yangtze River mouth to a major storm[J]. *Estuaries*, 2003, 26(6): 1416-1425.
- [11] 柏春广, 王建, 徐永辉. 江苏中部海岸全新世中期温暖期风暴潮频率的研究[J]. *海洋学报*, 2006, 28(6): 78-85.
Bo Chunguang, Wang Jian, Xu Yonghui. Researches on coastal storm surge frequency during the warm period of Middle Holocene in central Jiangsu Province in China[J]. *Haiyang Xuebao*, 2006, 28(6): 78-85.
- [12] 王爱军, 叶翔, 陈坚. 台风作用下的港湾型潮滩沉积过程——以2008年“凤凰”台风对福建省罗源湾的影响为例[J]. *海洋学报*, 2009, 31(6): 77-86.
Wang Aijun, Ye Xiang, Chen Jian. Effects of typhoon on sedimentary processes of embayment tidal flat—A case study from the “Fenghuang” typhoon in 2008[J]. *Haiyang Xuebao*, 2009, 31(6): 77-86.
- [13] Woodruff J D, Donnelly J P, Okusu A. Exploring typhoon variability over the mid-to-late Holocene: evidence of extreme coastal flooding from Kamikoshiki, Japan[J]. *Quaternary Science Reviews*, 2009, 28(17/18): 1774-1785.
- [14] Zhou Liang, Gao Shu, Yang Yang, et al. Typhoon events recorded in coastal lagoon deposits, southeastern Hainan Island[J]. *Acta Oceanologica Sinica*, 2017, 36(4): 37-45.
- [15] Williams H, Choowong M, Phantuwongraj S, et al. Geologic records of Holocene typhoon strikes on the Gulf of Thailand coast[J]. *Marine Geology*, 2016, 372: 66-78.
- [16] 陈联寿, 丁一汇. 西太平洋台风概论[M]. 北京: 科学出版社, 1979.
Chen Lianshou, Ding Yihui. Introduction to the Western Pacific Typhoons[M]. Beijing: Science Press, 1979.
- [17] Gray W M. Global view of the origin of tropical disturbances and storms[J]. *Monthly Weather Review*, 1968, 96(10): 669-700.
- [18] Gray W M. Hurricanes: Their formation, structure and likely role in the tropical circulation[M]//Shaw D B. *Meteorology Over the Tropical Oceans*. Bracknell: Royal Meteorological Society, James Glaisher House, Grenville Place, 1979: 155-218.
- [19] 马艳. 台风海面风场的动力分析、四维同化及数值试验[D]. 青岛: 中国科学院海洋研究所, 2000.
Ma Yan. Dynamical analyses, four-dimensional data assimilation and numerical experiment for typhoon sea surface wind[D]. Qingdao: Institute of Oceanology, Chinese Academy of Sciences, 2000.
- [20] 魏稳. 长江河口边滩多时间尺度动力地貌过程[D]. 上海: 华东师范大学, 2017.
Wei Wen. Multi-time-scale morphodynamics of the Changjiang estuarine marginal shoal[D]. Shanghai: East China Normal University, 2017.
- [21] Maio C V, Donnelly J P, Sullivan R, et al. Sediment dynamics and hydrographic conditions during storm passage, Waquoit Bay, Massachusetts[J]. *Marine Geology*, 2016, 381: 67-86.
- [22] Hung C W. A 300-year typhoon record in Taiwan and the relationship with solar activity[J]. *Terr. Terrestrial, Atmospheric and Oceanic Sciences*, 2013, 24(4): 737-743.
- [23] Mei W, Xie S P. Intensification of landfalling typhoons over the northwest Pacific since the late 1970s[J]. *Nature Geoscience*, 2016, 9(10): 753-757.
- [24] Wei Z J, Tang D L, Sui G J. An inferential statistical study on the climate characteristics of tropical cyclones over the Northwestern Pacific[M]//Tang D, Sui G. *Typhoon Impact and Crisis Management*. Berlin, Heidelberg: Springer, 2014: 333-349.
- [25] Peduzzi P, Chatenoux B, Dao H, et al. Global trends in tropical cyclone risk[J]. *Nature Climate Change*, 2012, 2(4): 289-294.
- [26] Webster P J, Holland G J, Curry J A, et al. Changes in tropical cyclone number, duration, and intensity in a warming environment[J].

- Science*, 2005, 309(5742): 1844–1846.
- [27] Mei Wei, Xie Shangping, Primeau F, et al. Northwestern Pacific typhoon intensity controlled by changes in ocean temperatures[J]. *Science Advances*, 2015, 1(4): e1500014.
- [28] Emanuel K A. The dependence of hurricane intensity on climate[J]. *Nature*, 1987, 326(6112): 483–485.
- [29] Knutson T R, Tuleya R E. Impact of CO₂-induced warming on simulated hurricane intensity and precipitation: Sensitivity to the choice of climate model and convective parameterization[J]. *Journal of Climate*, 2004, 17(18): 3477–3495.
- [30] Knutson T R, McBride J L, Chan J, et al. Tropical cyclones and climate change[J]. *Nature Geoscience*, 2010, 3(3): 157–163.
- [31] Liu K B, Shen Caiming, Louie K S. A 1, 000-Year history of typhoon landfalls in Guangdong, southern China, reconstructed from Chinese historical documentary records[J]. *Annals of the Association of American Geographers*, 2001, 91(3): 453–464.
- [32] García-Herrera R, Durán F R, Wheeler D, et al. The use of Spanish and British documentary sources in the investigation of Atlantic hurricane incidence in historical times[M]//Murphy R, Liu K B. *Hurricanes and Typhoons: Past, Present and Future*. New York: Columbia University Press, 2004.
- [33] Grossman M, Zaiki M. Reconstructing typhoons in Japan in the 1880s from documentary records[J]. *Weather*, 2009, 64(12): 315–322.
- [34] 王苏民, 刘健, 周静. 我国小冰期盛期的气候环境[J]. *湖泊科学*, 2003, 15(4): 369–376.
Wang Sumin, Liu Jian, Zhou Jing. The climate of Little Ice Age maximum in China[J]. *Journal of Lake Sciences*, 2003, 15(4): 369–376.
- [35] 陆人骥. 中国历代灾害性海潮史料[M]. 北京: 海洋出版社, 1984.
Lu Renji. *Compiling Data on Disastrous Storm Tides in Different Dynasties of China* [M]. Beijing: China Ocean Press, 1984.
- [36] 火恩杰, 刘昌森. 上海地区自然灾害史料汇编(公元751–1949年)[M]. 北京: 地震出版社, 2002.
Huo Enjie, Liu Changsen. *Compilation of Natural Disaster Data from 751 to 1949 in Shanghai* [M]. Beijing: Earthquake Press, 2002.
- [37] 张德二. 中国三千年气象记录总集[M]. 南京: 江苏教育出版社, 2004.
Zhang Deer. *A Compendium of Chinese Meteorological Records of the Last 3000 Year*[M]. Nanjing: Jiangsu Education Publishing House, 2004.
- [38] 梁有叶, 张德二. 最近一千年来我国的登陆台风及其与ENSO的关系[J]. *气候变化研究进展*, 2007, 3(2): 120–121.
Liang Youye, Zhang Deer. Landing typhoon in China during the last millennium and its relationship with ENSO[J]. *Advances in Climate Change Research*, 2007, 3(2): 120–121.
- [39] Louie K S, Liu K B. Earliest historical records of typhoons in China[J]. *Journal of Historical Geography*, 2003, 29(3): 299–316.
- [40] 王美苏. 清代入境中国东部沿海台风事件初步重建[D]. 上海: 复旦大学, 2010.
Wang Meisu. *A reconstruction of historical typhoon event invading the coast of East China from historical documentary: 1644–1911*[D]. Shanghai: Fudan University, 2010.
- [41] Zhang Xiangping, Ye Yu, Fang Xiuqi. Reconstruction of typhoons in the Yangtze River Delta during 1644–1949AD based on historical chorographies[J]. *Journal of Geographical Sciences*, 2012, 22(5): 810–824.
- [42] 徐明, 杨秋珍, 应明, 等. 影响华东台风 500 年历史资料重建方法[C]//2007年中国气象学会年会论文集. 北京: 气象出版社, 2007: 1000–1009.
Xu Ming, Yang Qiuzhen, Ying Ming, et al. Reconstruction method of 500 years historical typhoon data impacting East China[C]//Annual Meeting of China Meteorological Society in 2007. Beijing: China Meteorological Press, 2007: 1000–1009.
- [43] 潘威, 满志敏, 刘大伟, 等. 1644–1911年中国华东与华南沿海台风入境频率[J]. *地理研究*, 2014, 33(11): 2195–2204.
Pan Wei, Man Zhimin, Liu Dawei, et al. The changing of Chinese coastal typhoon frequency based on historical documents, 1644–1911AD[J]. *Geographical Research*, 2014, 33(11): 2195–2204.
- [44] 刘大伟. 清代入境中国南部沿海台风事件初步重建[D]. 上海: 复旦大学, 2013.
Liu Dawei. *Preliminary reconstruction of China's southern coastal typhoon events at Qing dynasty*[D]. Shanghai: Fudan University, 2013.
- [45] 日下部正雄. 史料からみた西日本の気象災害—第2報台风[J]. *天気*, 1960, 7(1): 16–21.
Kusakabe M. Historical review of meteorological damage in west part of Japan, II Typhoons[J]. *Tenki*, 1960, 7(1): 16–21.
- [46] 小西達男. 1828年シーボルト台風(子年の大風)と高潮[J]. *天気*, 2010, 57(6): 383–398.
Konishi T. Siebold typhoon in 1828 (Otherwise “Nenotoshi” Typhoon) and induced storm surges[J]. *Tenki*, 2010, 57(6): 383–398.
- [47] 周亮, 高抒, 杨阳, 等. 海南岛东南部海湾350年古风暴事件沉积与历史文献记录对比[J]. *海洋学报*, 2015, 37(9): 84–94.
Zhou Liang, Gao Shu, Yang Yang, et al. Comparison of paleostorm events between sedimentary and historical archives: A 350 year record from southeastern Hainan Island coastal embayments[J]. *Haiyang Xuebao*, 2015, 37(9): 84–94.
- [48] Schuerch M, Dolch T, Reise K, et al. Unravelling interactions between salt marsh evolution and sedimentary processes in the Wadden Sea (southeastern North Sea)[J]. *Progress in Physical Geography*, 2014, 38(6): 691–715.
- [49] 苗丽敏, 杨世伦, 朱琴, 等. 风暴过程中潮滩悬沙浓度和悬沙运输的变化及其动力机制——以长江三角洲南汇潮滩为例[J]. *海洋学报*, 2016, 38(5): 158–167.
Miao Limin, Yang Shilun, Zhu Qin, et al. Variations of suspended sediment concentrations and transport in response to a storm and its dynamic mechanism—A study case of Nanhui tidal flat of the Yangtze River Delta[J]. *Haiyang Xuebao*, 2016, 38(5): 158–167.
- [50] Rosencranz J A, Ganju N K, Ambrose R F, et al. Balanced sediment fluxes in Southern California's Mediterranean-climate zone salt

- marshes[J]. *Estuaries and Coasts*, 2016, 39(4): 1035–1049.
- [51] Janssen-Stelder B. The effect of different hydrodynamic conditions on the morphodynamics of a tidal mudflat in the Dutch Wadden Sea[J]. *Continental Shelf Research*, 2000, 20(12/13): 1461–1478.
- [52] Mariotti G. Revisiting salt marsh resilience to sea level rise: are ponds responsible for permanent land loss?[J]. *Journal of Geophysical Research: Earth Surface*, 2016, 121(7): 1391–1407.
- [53] Priestas A M, Mariotti G, Leonardi N, et al. Coupled wave energy and erosion dynamics along a salt marsh boundary, Hog Island Bay, Virginia, USA[J]. *Journal of Marine Science and Engineering*, 2015, 3(3): 1041–1065.
- [54] Xie Weiming, He Qing, Zhang Keqi, et al. Application of terrestrial laser scanner on tidal flat morphology at a typhoon event timescale[J]. *Geomorphology*, 2017, 292: 47–58.
- [55] Fagherazzi S, Carniello L, D'Alpaos L, et al. Critical bifurcation of shallow microtidal landforms in tidal flats and salt marshes[J]. *Proceedings of the National Academy of Sciences of the United States of America*, 2006, 103(22): 8337–8341.
- [56] Anthony E J. Storms, shoreface morphodynamics, sand supply, and the accretion and erosion of coastal dune barriers in the southern North Sea[J]. *Geomorphology*, 2013, 199: 8–21.
- [57] Hill H W, Kelley J T, Belknap D F, et al. The effects of storms and storm-generated currents on sand beaches in southern Maine, USA[J]. *Marine Geology*, 2004, 210(1/4): 149–168.
- [58] Short A D. Beach systems of the central netherlands coast: processes, morphology and structural impacts in a storm driven multi-bar system[J]. *Marine Geology*, 1992, 107(1/2): 103–137.
- [59] Castelle B, Bonneton P, Dupuis H, et al. Double bar beach dynamics on the high-energy meso-macrotidal french aquitanian coast: a review[J]. *Marine Geology*, 2007, 245(1/4): 141–159.
- [60] Dissanayake P, Brown J, Karunarathna H. Impacts of storm chronology on the morphological changes of the formby beach and dune system, UK[J]. *Natural Hazards and Earth System Sciences*, 2015, 15(7): 1533–1543.
- [61] 戴志军, 陈子燊, 李春初. 岬间海滩剖面短期变化的动力作用分析[J]. *海洋科学*, 2001, 25(11): 38–41.
Dai Zhijun, Chen Zishen, Li Chunchu. Analysis of dynamical actions on the process of beach profile between headlands over a short time[J]. *Marine Sciences*, 2001, 25(11): 38–41.
- [62] 蔡锋, 苏贤泽, 曹惠美, 等. 华南砂质海滩的动力地貌分析[J]. *海洋学报*, 2005, 27(2): 106–114.
Cai Feng, Su Xianze, Cao Huimei, et al. Analysis on morphodynamics of sandy beaches in South China[J]. *Haiyang Xuebao*, 2005, 27(2): 106–114.
- [63] Sallenger A H Jr. Storm impact scale for barrier islands[J]. *Journal of Coastal Research*, 2000, 16(3): 890–895.
- [64] Reading H G. *Sedimentary Environments and Facies*[M]. 2nd ed. Oxford: Blackwell Scientific Publications, 1986: 615.
- [65] Zhou Liang, Yang Yang, Wang Zhanghua, et al. Investigating ENSO and WPWP modulated typhoon variability in the South China Sea during the mid-late Holocene using sedimentological evidence from southeastern Hainan Island, China[J]. *Marine Geology*, 2019, 416: 105987.
- [66] Sakuna-Schwartz D, Feldens P, Schwarzer K, et al. Internal structure of event layers preserved on the Andaman Sea continental shelf, Thailand: tsunami vs. storm and flash-flood deposits[J]. *Natural Hazards and Earth System Sciences*, 2015, 15(6): 1181–1199.
- [67] Cunningham A C, Bakker M A J, Van Heteren S, et al. Extracting storm-surge data from coastal dunes for improved assessment of flood risk[J]. *Geology*, 2011, 39(11): 1063–1066.
- [68] 王建, 柏春广, 徐永辉. 江苏中部淤泥质滩涂潮汐层成因机理和风暴沉积判别标志[J]. *沉积学报*, 2006, 24(4): 562–569.
Wang Jian, Bo Chunguang, Xu Yonghui. Mechanism of silt-mud couplet of mud tidal flat and discrimination criteria of storm surge sedimentation in the middle Jiangsu Province[J]. *Acta Sedimentologica Sinica*, 2006, 24(4): 562–569.
- [69] Liu K B. Paleotempestology[M]//Elias S C. *Encyclopedia of Quaternary Science*. Amsterdam: Elsevier, 2006.
- [70] Rankey E C, Enos P, Steffen K, et al. Lack of impact of hurricane Michelle on tidal flats, Andros island, Bahamas: integrated remote sensing and field observations[J]. *Journal of Sedimentary Research*, 2004, 74(5): 654–661.
- [71] 赵秧秧, 高抒. 台风风暴潮影响下滩涂沉积动力模拟初探——以江苏如东海岸为例[J]. *沉积学报*, 2015, 33(1): 79–90.
Zhao Yangyang, Gao Shu. Simulation of tidal flat sedimentation in response to typhoon-induced storm surges: a case study from Rudong coast, Jiangsu, China[J]. *Acta Sedimentologica Sinica*, 2015, 33(1): 79–90.
- [72] Harms J C, Southard J B, Spearing D R, et al. *Depositional Environments as Interpreted from Primary Sedimentary Structures and Stratification Sequence*[M]. Texas: Society of Economic Paleontologists and Mineralogists, 1975: 161.
- [73] Lambert W J, Aharon P, Rodriguez A B. Catastrophic hurricane history revealed by organic geochemical proxies in coastal lake sediments: a case study of Lake Shelby, Alabama (USA)[J]. *Journal of Paleolimnology*, 2008, 39(1): 117–131.
- [74] Williams H F L. 600-year sedimentary archive of hurricane strikes in a prograding beach ridge plain, southwestern Louisiana[J]. *Marine Geology*, 2013, 336: 170–183.
- [75] Wallace D J, Woodruff J D, Anderson J B, et al. Palaeohurricane reconstructions from sedimentary archives along the Gulf of Mexico, Caribbean Sea and western North Atlantic Ocean margins[J]. *Geological Society, London, Special Publications*, 2014, 388(1): 481–501.
- [76] Zhao Yifei, Zou Xinqing, Gao Jianhua, et al. Recent sedimentary record of storms and floods within the estuarine-inner shelf region of the East China Sea[J]. *The Holocene*, 2016, 27(3): 439–449.

- [77] Smith T A, Chen S, Campbell T, et al. Ocean-wave coupled modeling in COAMPS-TC: A study of Hurricane Ivan (2004)[J]. *Ocean Modelling*, 2013, 69(2): 181–194.
- [78] 田元, 范德江, 张喜林, 等. 东海内陆架沉积物敏感粒级构成及其地质意义[J]. *海洋与湖沼*, 2016, 47(2): 30–37.
Tian Yuan, Fan Dejiang, Zhang Xilin. Sensitive grain size components and their geological implication in the inner shelf of the East China Sea[J]. *Oceanologia et Limnologia Sinica*, 2016, 47(2): 30–37.
- [79] Jia Jianjun, Gao Jianhua, Cai Tinglu, et al. Sediment accumulation and retention of the Changjiang (Yangtze River) subaqueous delta and its distal muds over the last century[J]. *Marine Geology*, 2018, 401: 2–16.
- [80] Gao Jianhua, Shi Yong, Sheng Hui, et al. Rapid response of the Changjiang (Yangtze) River and East China Sea source-to-sink conveying system to human induced catchment perturbations[J]. *Marine Geology*, 2019, 414: 1–17.
- [81] Xiao Shangbin, Li Anchun, Jiang Fuqing, et al. Recent 2000-year geological records of mud in the inner shelf of the East China Sea and their climatic implications[J]. *Chinese Science Bulletin*, 2005, 50(5): 466–471.
- [82] Li Yuhai, Wang Aijun, Qiao Lei, et al. The impact of typhoon Morakot on the modern sedimentary environment of the mud deposition center off the Zhejiang–Fujian coast, China[J]. *Continental Shelf Research*, 2012, 37: 92–100.
- [83] Gao Shu, Liu Yunling, Yang Yang, et al. Evolution status of the distal mud deposit associated with the Pearl River, northern South China Sea continental shelf[J]. *Journal of Asian Earth Sciences*, 2015, 114: 562–573.
- [84] 任美锷, 张忍顺, 杨巨海. 江苏王港地区淤泥质潮滩的沉积作用[J]. *海洋通报*, 1984, 3(1): 40–52.
Ren Meie, Zhang Renshun, Yang Juhai. Sedimentation on tidal mud flat in Wanggang area, Jiangsu Province, China[J]. *Marine Science Bulletin*, 1984, 3(1): 40–52.
- [85] 许世远, 邵虚生, 陈中原, 等. 长江三角洲风暴沉积系列研究[J]. *中国科学: B辑*, 1990, 33(10): 1242–1250.
Xu Shiyan, Shao Xusheng, Chen Zhongyuan, et al. Storm deposits in the Changjiang delta[J]. *Science in China: Series B*, 1990, 33(10): 1242–1250.
- [86] Shao X S, Yan Q S, Xu S Y, et al. Storm deposits in the coastal region of Shanghai, the Yangtze Delta, China[J]. *Geologie en Mijnbouw*, 1991, 70: 45–58.
- [87] 张国栋, 王益友, 朱静昌, 等. 现代滨岸风暴沉积——以舟山普陀岛、朱家尖岛为例[J]. *沉积学报*, 1987, 5(2): 17–28.
Zhang Guodong, Wang Yiyu, Zhu Jingchang, et al. Modern coastal storm deposits of Putuo Island and Zhujiajian Island, Zhoushan[J]. *Acta Sedimentologica Sinica*, 1987, 5(2): 17–28.
- [88] 陈卫跃. 潮滩泥沙输移及沉积动力环境——以杭州湾北岸、长江口南岸部分潮滩为例[J]. *海洋学报*, 1991, 13(6): 813–821.
Chen Weiyue. Sediment dynamics and transport in tidal flat: A case study of the north Hangzhou Bay and south Yangtze River estuary[J]. *Haiyang Xuebao*, 1991, 13(6): 813–821.
- [89] Ren Meie, Zhang Renshun, Yang Juhai. Effect of typhoon no. 8114 on coastal morphology and sedimentation of Jiangsu Province, People's Republic of China[J]. *Journal of Coastal Research*, 1985, 1(1): 21–28.
- [90] Gao Shu. Modeling the preservation potential of tidal flat sedimentary records, Jiangsu coast, eastern China[J]. *Continental Shelf Research*, 2009, 29(16): 1927–1936.
- [91] Liu K B. Paleotempestology: Principles, methods, and examples from gulf coast lake-sediments[M]//Murnane R J, Liu K B. *Hurricanes and Typhoons: Past, Present, and Future*. New York: Columbia University Press, 2004: 13–57.
- [92] 黄光庆, 严维枢. 有孔虫指示的珠江口全新世风暴潮沉积信息[J]. *科学通报*, 1997, 42(4): 423–426.
Huang Guangqing, Yan Weishu. Holocene storm deposits information of the Pearl estuary indicated by foraminifera[J]. *Chinese Science Bulletin*, 1997, 42(4): 423–426.
- [93] Collins E S, Scott D B, Gayes P T. Hurricane records on the South Carolina coast: Can they be detected in the sediment record?[J]. *Quaternary International*, 1999, 56(1): 15–26.
- [94] Nott J. Palaeotempestology: the study of prehistoric tropical cyclones—a review and implications for hazard assessment[J]. *Environment International*, 2004, 30(3): 433–447.
- [95] Katsuki K, Yang D Y, Seto K, et al. Factors controlling typhoons and storm rain on the Korean Peninsula during the Little Ice Age[J]. *Journal of Paleolimnology*, 2016, 55(1): 35–48.
- [96] Chen H F, Wen S Y, Song Senrong, et al. Strengthening of paleo-typhoon and autumn rainfall in Taiwan corresponding to the Southern Oscillation at late Holocene[J]. *Journal of Quaternary Science*, 2012, 27(9): 964–972.
- [97] Donnelly C, Kraus N, Larson M. State of knowledge on measurement and modeling of coastal overwash[J]. *Journal of Coastal Research*, 2006, 22(4): 965–991.
- [98] King C A M. *Beaches and Coasts*[M]. 2nd ed. London: Palgrave Macmillan, 1972: 570.
- [99] Shaw J, You Yao, Mohrig D, et al. Tracking hurricane-generated storm surge with washover fan stratigraphy[J]. *Geology*, 2015, 43(2): 127–130.
- [100] Phantuwongraj S, Choowong M, Nanayama F, et al. Coastal geomorphic conditions and styles of storm surge washover deposits from Southern Thailand[J]. *Geomorphology*, 2013, 192: 43–58.
- [101] Wang Ping, Horwitz M H. Erosional and depositional characteristics of regional overwash deposits caused by multiple hurricanes[J]. *Sedimentology*, 2007, 54(3): 545–564.

- [102] 杨保明, 高抒, 周亮, 等. 海南岛东南部海岸砂丘风暴冲越沉积记录[J]. 沉积学报, 2017, 35(6): 1133–1143.
Yang Baoming, Gao Shu, Zhou Liang, et al. A coastal dune overwash record of typhoon storm events from southeastern Hainan Island[J]. *Acta Sedimentologica Sinica*, 2017, 35(6): 1133–1143.
- [103] Nott J F. Extremely high-energy wave deposits inside the Great Barrier Reef, Australia: determining the cause—tsunami or tropical cyclone[J]. *Marine Geology*, 1997, 141(1/4): 193–207.
- [104] Frohlich C, Hornbach M J, Taylor F W, et al. Huge erratic boulders in Tonga deposited by a prehistoric tsunami[J]. *Geology*, 2009, 37(2): 131–134.
- [105] Kennedy A B, Mori N, Yasuda T, et al. Extreme block and boulder transport along a cliffed coastline (Calicoan Island, Philippines) during Super Typhoon Haiyan[J]. *Marine Geology*, 2017, 383: 65–77.
- [106] Scheffers A. Tsunami boulder deposits[M]//Shiki T, Tsuji Y, Yamazaki T, et al. Tsunamiites. Features and Implications. Amsterdam: Elsevier, 2008: 299–317.
- [107] Goto K, Kawana T, Imamura F. Historical and geological evidence of boulders deposited by tsunamis, southern Ryukyu Islands, Japan[J]. *Earth-Science Reviews*, 2010, 102(1/2): 77–99.
- [108] Dawson A G, Stewart I, Morton R A, et al. Reply to comments by Kelletat (2008) Comments to Dawson, A. G. and Stewart, I. Tsunami deposits in the geological record[J]. *Sedimentary Geology*, 2008, 211(3/4): 92–93.
- [109] Goto K, Miyagi K, Kawana T, et al. Emplacement and movement of boulders by known storm waves—field evidence from the Okinawa Islands, Japan[J]. *Marine Geology*, 2011, 283(1/4): 66–78.
- [110] Nandasena N A K, Paris R, Tanaka N. Reassessment of hydrodynamic equations: minimum flow velocity to initiate boulder transport by high energy events (storms, tsunamis)[J]. *Marine Geology*, 2011, 281(1/4): 70–84.
- [111] Hongo C, Kurihara H, Golbuu Y. Coral boulders on Melekeok reef in the Palau Islands: An indicator of wave activity associated with tropical cyclones[J]. *Marine Geology*, 2018, 399: 14–22.
- [112] Mastroruzzi G, Pignatelli C. The boulder berm of Punta Saguerra (Taranto, Italy): a morphological imprint of the Rossano Calabro tsunami of April 24, 1836?[J]. *Earth, Planets and Space*, 2012, 64(10): 829–842.
- [113] Hoffmeister D, Ntageretzis K, Aasen H, et al. 3D model-based estimations of volume and mass of high-energy dislocated boulders in coastal areas of Greece by terrestrial laser scanning[J]. *Zeitschrift für Geomorphologie, Supplementary Issues*, 2014, 58(3): 115–135.
- [114] Telling J, Lyda A, Hartzell P, et al. Review of Earth science research using terrestrial laser scanning[J]. *Earth-Science Reviews*, 2017, 169: 35–68.
- [115] Roig-Munar F X, Rodríguez-Perea A, Vilaplana J M, et al. Tsunami boulders in Majorca Island (Balearic Islands, Spain)[J]. *Geomorphology*, 2019, 334: 76–90.
- [116] Kennedy D M, Woods J L D, Naylor L A, et al. Intertidal boulder-based wave hindcasting can underestimate wave size: Evidence from Yorkshire, UK[J]. *Marine Geology*, 2019, 411: 98–106.
- [117] Hastewell L J, Schaefer M, Bray M, et al. Intertidal boulder transport: A proposed methodology adopting Radio Frequency Identification (RFID) technology to quantify storm induced boulder mobility[J]. *Earth Surface Processes and Landforms*, 2019, 44(3): 681–698.
- [118] Gandhi D, Chavare K A, Prizomwala S P, et al. Testing the numerical models for boulder transport through high energy marine wave event: An example from southern Saurashtra, western India[J]. *Quaternary International*, 2017, 444: 209–216.
- [119] Herterich J G, Cox R, Dias F. How does wave impact generate large boulders? Modelling hydraulic fracture of cliffs and shore platforms[J]. *Marine Geology*, 2018, 399: 34–46.
- [120] 徐笑梅, 高抒, 周亮, 等. 海南岛东北部海岸极端波浪事件沉积记录[J]. 海洋学报, 2019, 41(6): 48–63.
Xu Xiaomei, Gao Shu, Zhou Liang, et al. Sedimentary records of extreme wave events on the northeastern Hainan Island coast, southern China[J]. *Haiyang Xuebao*, 2019, 41(6): 48–63.
- [121] Wheatcroft R A, Drake D E. Post-depositional alteration and preservation of sedimentary event layers on continental margins, I. The role of episodic sedimentation[J]. *Marine Geology*, 2003, 199(1/2): 123–137.
- [122] Hippensteel S P. Preservation potential of storm deposits in South Carolina back-barrier marshes[J]. *Journal of Coastal Research*, 2008, 243: 594–601.
- [123] Hart M. Evaluating the preservation of hurricane deposits in Florida coastal sediments[D]. Gainesville: University of Florida, 2003.
- [124] Liu K B, Li C, Bianchette T A, et al. Storm deposition in a coastal backbarrier lake in Louisiana caused by Hurricanes Gustav and Ike[J]. *Journal of Coastal Research*, 2011, 64: 1866–1870.
- [125] Tamura T. Beach ridges and prograded beach deposits as palaeoenvironment records[J]. *Earth-Science Reviews*, 2012, 114(3/4): 279–297.
- [126] Toomey M, Cantwell M, Colman S, et al. The mighty Susquehanna—extreme floods in Eastern North America during the past two millennia[J]. *Geophysical Research Letters*, 2019, 46(6): 3398–3407.
- [127] Kreisa R D. Storm-generated sedimentary structures in subtidal marine facies with examples from the Middle and Upper Ordovician of southwestern Virginia[J]. *Journal of Sedimentary Research*, 1981, 51(3): 823–848.
- [128] 严钦尚. 论滨岸和浅海的风暴沉积[J]. 海洋与湖沼, 1984, 15(1): 14–20.
Yan Qinshang. Overview of the storm-generated deposits on nearshore zone and open shelf[J]. *Oceanologia et Limnologia Sinica*, 1984,

- 15(1): 14–20.
- [129] Liu K B, Fearn M L. Lake-sediment record of late Holocene hurricane activities from coastal Alabama[J]. *Geology*, 1993, 21(9): 793–796.
- [130] Bregy J C, Wallace D J, Minzoni R T, et al. 2500-year paleotempestological record of intense storms for the northern Gulf of Mexico, United States[J]. *Marine Geology*, 2018, 396: 26–42.
- [131] Yu Kefu, Zhao Jianxin, Collerson K D, et al. Storm cycles in the last millennium recorded in Yongshu Reef, southern South China Sea[J]. *Palaeogeography, Palaeoclimatology, Palaeoecology*, 2004, 210(1): 89–100.
- [132] Cox R, Jahn K L, Watkins O G, et al. Extraordinary boulder transport by storm waves(West of Ireland, Winter 2013–2014), and criteria for analysing coastal boulder deposits[J]. *Earth-Science Reviews*, 2018, 177: 623–636.
- [133] 王为, 李平日, 谭惠忠, 等. 南海北部长湾风暴潮贝壳堤的沉积特征及发育模式[J]. *地质学报*, 2010, 84(12): 1829–1838.
Wang Wei, Li Pingri, Tan Huizhong, et al. Depositional characteristics and development model of a chenier built up by storm surges on the coast of the northern South China Sea[J]. *Acta Geologica Sinica*, 2010, 84(12): 1829–1838.
- [134] Nott J F, Forsyth A, Rhodes E, et al. The origin of centennial-to millennial-scale chronological gaps in storm emplaced beach ridge plains[J]. *Marine Geology*, 2015, 367: 83–93.
- [135] Allison M A, Sheremet A, Goñi M A, et al. Storm layer deposition on the Mississippi–Atchafalaya subaqueous delta generated by Hurricane Lili in 2002[J]. *Continental Shelf Research*, 2005, 25(18): 2213–2232.
- [136] Wang Jian, Bai Chunguang, Xu Yonghui, et al. Tidal couplet formation and preservation, and criteria for discriminating storm-surge sedimentation on the tidal flats of central Jiangsu Province, China[J]. *Journal of Coastal Research*, 2010, 26(5): 976–981.
- [137] Hamblin A P, Duke W L, Walker R G. Hummocky cross-stratification—indicator of storm-dominated shallow-marine environments[J]. *AAPG Bulletin*, 1979, 63(3): 460–461.
- [138] Hong I, Pilarczyk J E, Horton B P, et al. Sedimentological characteristics of the 2015 Tropical Cyclone Pam overwash sediments from Vanuatu, South Pacific[J]. *Marine Geology*, 2018, 396: 205–214.
- [139] Nott J F. Intensity of prehistoric tropical cyclones[J]. *Journal of Geophysical Research*, 2003, 108(D7): 4212.
- [140] 王为, 谭惠忠. 贝壳堤的形成与风暴沉积——以广东台山长湾贝壳堤为例[J]. *热带地理*, 2003, 23(3): 209–213.
Wang Wei, Tan Huizhong. Formation of a chenier and storm deposits—A case study of the coast of south China[J]. *Tropical Geography*, 2003, 23(3): 209–213.
- [141] 王强, 袁桂邦, 张熟, 等. 渤海湾西岸贝壳堤堆积与海陆相互作用[J]. *第四纪研究*, 2007, 27(5): 775–786.
Wang Qiang, Yuan Guibang, Zhang Shu, et al. Shelly ridge accumulation and sea-land interaction on the west coast of the Bohai Bay[J]. *Quaternary Sciences*, 2007, 27(5): 775–786.
- [142] Goto K, Okada K, Imamura F. Characteristics and hydrodynamics of boulders transported by storm waves at Kudaka Island, Japan[J]. *Marine Geology*, 2009, 262(1/4): 14–24.
- [143] Terry J P, Oliver G J H, Friess D A. Ancient high-energy storm boulder deposits on Ko Samui, Thailand, and their significance for identifying coastal hazard risk[J]. *Palaeogeography, Palaeoclimatology, Palaeoecology*, 2016, 454: 282–293.
- [144] Schwartz R K. Bedform and stratification characteristics of some modern small-scale washover sand bodies[J]. *Sedimentology*, 1982, 29(6): 835–849.
- [145] 李平日, 黄光庆, 谭惠忠, 等. 珠江口地区风暴潮沉积的研究[M]. 广州: 广东科技出版社, 2002: 153.
Li Pingri, Huang Guangqing, Tan Huizhong, et al. Storm Sedimentation in the Pearl River Estuary[M]. Guangzhou: Guangdong Science & Technology Press, 2002: 153.
- [146] 高抒. 海洋沉积动力学研究导引[M]. 南京: 南京大学出版社, 2013: 398.
Gao Shu. Introduction to Marine Sedimentary Dynamics[M]. Nanjing: Nanjing University Press, 2013: 398.
- [147] Nanayama F, Shigeno K, Satake K, et al. Sedimentary differences between the 1993 Hokkaido-nansei-oki tsunami and the 1959 Miyakojima typhoon at Taisei, southwestern Hokkaido, northern Japan[J]. *Sedimentary Geology*, 2000, 135(1/4): 255–264.
- [148] Zhang Erfeng, Gao Shu, Savenije H H G, et al. Saline water intrusion in relation to strong winds during winter cold outbreaks: North Branch of the Yangtze Estuary[J]. *Journal of Hydrology*, 2019, 574: 1099–1109.
- [149] Fan Dejiang, Qi Hongyan, Sun Xiaoxia, et al. Annual lamination and its sedimentary implications in the Yangtze River delta inferred from high-resolution biogenic silica and sensitive grain-size records[J]. *Continental Shelf Research*, 2011, 31(2): 129–137.
- [150] Meyers P A. Preservation of elemental and isotopic source identification of sedimentary organic matter[J]. *Chemical Geology*, 1994, 114(3/4): 289–302.
- [151] Horowitz A J, Elrick K A, Smith J J, et al. The effects of hurricane Irene and tropical storm Lee on the bed sediment geochemistry of U. S. Atlantic coastal rivers[J]. *Hydrological Processes*, 2014, 28(3): 1250–1259.
- [152] Morton R A, Gelfenbaum G, Jaffe B E. Physical criteria for distinguishing sandy tsunami and storm deposits using modern examples[J]. *Sedimentary Geology*, 2007, 200(3/4): 184–207.
- [153] Yue Yuanfu, Yu Kefu, Tao Shichen, et al. 3500-year western Pacific storm record warns of additional storm activity in a warming warm pool[J]. *Palaeogeography, Palaeoclimatology, Palaeoecology*, 2019, 521: 57–71.
- [154] Kortekaas S, Dawson A G. Distinguishing tsunami and storm deposits: an example from Martinhal, SW Portugal[J]. *Sedimentary Geo-*

- logy, 2007, 200(3/4): 208–221.
- [155] Phantuwongraj S, Choowong M. Tsunamis versus storm deposits from Thailand[J]. *Natural Hazards*, 2012, 63(1): 31–50.
- [156] Sun Liguang, Zhou Xin, Huang Wen, et al. Preliminary evidence for a 1 000-year-old tsunami in the South China Sea[J]. *Scientific Reports*, 2013, 3: 1655.
- [157] 杨文卿, 孙立广, 杨仲康, 等. 南澳宋城: 被海啸毁灭的古文明遗址[J]. *科学通报*, 2019, 64(1): 107–120.
Yang Wenqing, Sun Liguang, Yang Zhongkang, et al. Nan'ao, an archaeological site of Song dynasty destroyed by tsunami[J]. *Chinese Science Bulletin*, 2019, 64(1): 107–120.
- [158] Goto K, Hashimoto K, Sugawara D, et al. Spatial thickness variability of the 2011 Tohoku-oki tsunami deposits along the coastline of Sendai Bay[J]. *Marine Geology*, 2014, 358: 38–48.
- [159] Chagué-Goff C, Szczuciński W, Shinozaki T. Applications of geochemistry in tsunami research: a review[J]. *Earth-Science Reviews*, 2017, 165: 203–244.
- [160] Somboonna N, Wilantho A, Jankaew K, et al. Microbial ecology of Thailand tsunami and non-tsunami affected terrestrials[J]. *PLoS One*, 2014, 9(4): e94236.
- [161] Rubin C M, Horton B P, Sieh K, et al. Highly variable recurrence of tsunamis in the 7400 years before the 2004 Indian Ocean tsunami[J]. *Nature Communications*, 2017, 8: 16019.
- [162] Rydgren K, Bondevik S. Moss growth patterns and timing of human exposure to a Mesolithic tsunami in the North Atlantic[J]. *Geology*, 2015, 43(2): 111–114.
- [163] Nandasena N A K, Tanaka N, Sasaki Y, et al. Boulder transport by the 2011 Great East Japan tsunami: Comprehensive field observations and whether model predictions?[J]. *Marine Geology*, 2013, 346: 292–309.
- [164] Liu K B, Fearn M L. Reconstruction of prehistoric landfall frequencies of catastrophic hurricanes in northwestern Florida from lake sediment records[J]. *Quaternary Research*, 2000, 54(2): 238–245.
- [165] Elsner J B, Jagger T H, Liu K B. Comparison of hurricane return levels using historical and geological records[J]. *Journal of Applied Meteorology and Climatology*, 2008, 47(2): 368–374.
- [166] Nott J F, Forsyth A. Punctuated global tropical cyclone activity over the past 5000 years[J]. *Geophysical Research Letters*, 2012, 39(14): L14703.
- [167] Woodruff J D, Donnelly J P, Mohrig D, et al. Reconstructing relative flooding intensities responsible for hurricane-induced deposits from Laguna Playa Grande, Vieques, Puerto Rico[J]. *Geology*, 2008, 36(5): 391–394.
- [168] Brandon C M, Woodruff J D, Donnelly J P, et al. How unique was Hurricane Sandy? Sedimentary reconstructions of extreme flooding from New York Harbor[J]. *Scientific Reports*, 2014, 4: 7366.
- [169] Stockdon H F, Holman R A, Howd P A, et al. Empirical parameterization of setup, swash, and runup[J]. *Coastal Engineering*, 2006, 53(7): 573–588.
- [170] Brandon C M, Woodruff J D, Lane D, et al. Tropical cyclone wind speed constraints from resultant storm surge deposition: A 2500 year reconstruction of hurricane activity from St. Marks, FL[J]. *Geochemistry, Geophysics, Geosystems*, 2013, 14(8): 2993–3008.
- [171] Laigle L, Joseph P, De Marsily G, et al. 3-D process modelling of ancient storm-dominated deposits by an event-based approach: Application to Pleistocene-to-modern Gulf of Lions deposits[J]. *Marine Geology*, 2013, 335: 177–199.
- [172] Gao S, Collins M B. Holocene sedimentary systems on continental shelves[J]. *Marine Geology*, 2014, 352: 268–294.
- [173] Huang C S Y, Nakamura N. Local wave activity budgets of the wintertime Northern Hemisphere: Implication for the Pacific and Atlantic storm tracks[J]. *Geophysical Research Letters*, 2017, 44(11): 5673–5682.
- [174] Stark, J, Smolders S, Meire P, et al. Impact of intertidal area characteristics on estuarine tidal hydrodynamics: a modelling study for the Scheldt Estuary[J]. *Estuarine, Coastal and Shelf Science*, 2017, 198: 138–155.
- [175] Hu Kelin, Ding Pingxing, Wang Zhengbing, et al. A 2D/3D hydrodynamic and sediment transport model for the Yangtze Estuary, China[J]. *Journal of Marine Systems*, 2009, 77(1/2): 114–136.
- [176] Hu Kelin, Chen Qin, Wang Hongqing, et al. Numerical modeling of salt marsh morphological change induced by Hurricane Sandy[J]. *Coastal Engineering*, 2018, 132: 63–81.
- [177] Goldenberg S B, Landsea C W, Mestas-Nuñez A M, et al. The recent increase in Atlantic hurricane activity: Causes and implications[J]. *Science*, 2001, 293(5529): 474–479.
- [178] Chan J C L. Comment on “Changes in tropical cyclone number, duration, and intensity in a warming environment”[J]. *Science*, 2006, 311(5768): 1713.
- [179] Elsner J B, Kossin J P, Jagger T H. The increasing intensity of the strongest tropical cyclones[J]. *Nature*, 2008, 455(7209): 92–95.
- [180] Sobel A H, Camargo S J, Hall T M, et al. Human influence on tropical cyclone intensity[J]. *Science*, 2016, 353(6296): 242–246.
- [181] Bhatia K T, Vecchi G A, Knutson T R, et al. Recent increases in tropical cyclone intensification rates[J]. *Nature Communications*, 2019, 10: 635.
- [182] Emanuel K A. Downscaling CMIP5 climate models shows increased tropical cyclone activity over the 21st century[J]. *Proceedings of the National Academy of Sciences of the United States of America*, 2013, 110(30): 12219–12224.
- [183] Bacmeister J T, Reed K A, Hannay C, et al. Projected changes in tropical cyclone activity under future warming scenarios using a high-

- resolution climate model[J]. *Climatic Change*, 2018, 146(3/4): 547–560.
- [184] 王宏, 李建芬, 裴艳东, 等. 渤海湾西岸海岸带第四纪地质研究成果概述[J]. *地质调查与研究*, 2011, 34(2): 81–97.
Wang Hong, Li Jianfen, Pei Yandong, et al. Study of Quaternary geology on the west coast of Bohai Bay[J]. *Geological Survey and Research*, 2011, 34(2): 81–97.
- [185] Chen H F, Liu Y C, Chiang C W, et al. China's historical record when searching for tropical cyclones corresponding to Intertropical Convergence Zone(ITCZ) shifts over the past 2 kyr[J]. *Climate of the Past*, 2019, 15(1): 279–289.
- [186] Donnelly J P, Hawkes A D, Lane P, et al. Climate forcing of unprecedented intense - hurricane activity in the last 2000 years[J]. *Earth's Future*, 2015, 3(2): 49–65.
- [187] Moy C M, Seltzer G O, Rodbell D T, et al. Variability of El Niño/Southern oscillation activity at millennial timescales during the Holocene epoch[J]. *Nature*, 2002, 420(6912): 162–165.
- [188] 顾成林, 康建成, 闫国东, 等. 1951–2015年登陆中国热带气旋的时空变化特征及与ENSO的关系[J]. *灾害学*, 2018, 33(4): 129–134, 140.
Gu Chenglin, Kang Jiancheng, Yan Guodong, et al. Spatial and temporal variations of tropical cyclones landing on China in 1951–2015 and their relationship with ENSO[J]. *Journal of Catastrophology*, 2018, 33(4): 129–134, 140.
- [189] 王会军, 范可, 孙建奇, 等. 关于西太平洋台风气候变异和预测的若干研究进展[J]. *大气科学*, 2007, 31(6): 1076–1081.
Wang Huijun, Fan Ke, Sun Jianqi, et al. Some advances in the researches of the western north Pacific typhoon climate variability and prediction[J]. *Chinese Journal of Atmospheric Sciences*, 2007, 31(6): 1076–1081.
- [190] Tu J Y, Chou C, Chu P S. The abrupt shift of typhoon activity in the vicinity of Taiwan and its association with western North Pacific–East Asian climate change[J]. *Journal of Climate*, 2009, 22(13): 3617–3628.

Obtaining typhoon information from sedimentary records in coastal-shelf waters

Gao Shu¹, Jia Jianjun¹, Yang Yang¹, Zhou Liang¹, Wei Wen¹, Mei Yanjun¹, Li Ya'nan¹,
Wang Li¹, Zhao Peipei¹, Liu Zhenqiao¹, Zhang Lifen¹

(1. State Key Laboratory of Estuarine and Coastal Research, School of Marine Sciences, East China Normal University, Shanghai 200241, China)

Abstract: The typhoon intensity-frequency relationship over a long period of time is related to climate change, but it is difficult to provide sufficient information from instrumental and historical records. Therefore, to extract storm information from sedimentary records has become a critical scientific problem; the solution to the problem can provide a decision-making basis for coastal cities to cope with future climate and sea level changes. The present study on the progress in the research of typhoon sedimentary records shows that shelf mud deposits, beaches and coastal dunes, tidal flats, lagoons and storm boulders contain records of extreme events. These event layers can be identified by stratigraphic sequence features and sediment characteristics. Typhoon records along the coastline of China have been found in large quantities, but further improvements to the information-obtaining methodology are needed to distinguish between deposits of typhoons, winter outbreaks, river floods and tsunami events. Thus, in terms of the information on typhoon intensity in shelf muds, coarse-grained and shell particles in the deposits can be used as indicators of intensity of bottom resuspension, but calibration with sufficient measurements is required. The elevation of typhoon deposit on the top of beaches and coastal dunes may indicate the height of swash during a typhoon event, while the size of storm boulders has a significant correlation with the offshore wave height. These data can be used to deduce typhoon intensity, although they are not enough to establish the intensity-frequency relationship. Tidal flat and lagoon deposits have a high continuity and can be used to reconstruct the time series of typhoon events. However, the solution to typhoon intensity is not unique because different combinations of maximum wind speed, path, landing place and duration may produce the same event deposit. We propose that a new method of obtaining typhoon information should be developed to solve this problem. Numerical simulation of modern

process, with the help and assimilation of available data and knowledge of typhoon events, would be useful to reproduce the characteristics of event deposits. Then, inverse simulation for event deposits can be carried out for multiple locations, to constrain the solution domain. This method may be referred to as "solution domain constraining method". The uncertainty can be further reduced by means of big data analysis, i.e., incorporating other dataset of typhoon intensity into the simulation system. A combination of dynamic process simulation and big data treatment is helpful to the establishment of the intensity-frequency curve of typhoon with the same time scale as the sedimentary record; on such a basis, the relationship between typhoon variation and climate change can be analyzed.

Key words: typhoon processes; event deposits; intensity-frequency relationship; sediment dynamic simulation; solution domain constraining method; coast and shelf waters